





Solar Energy

Numerical device modeling for direct Z-scheme junctions using a solar cell simulator --Manuscript Draft--

Manuscript Number:	SEJ-D-23-00779R1
Article Type:	Research paper
Section/Category:	Other solar energy topics
Keywords:	Semiconductor; Catalysis; Simulations; Modelling; Photocatalysis; Electrocatalysis
Corresponding Author:	Nithin Thomas Jacob, Master in Science Ghent University Ghent, BELGIUM
First Author:	Nithin Thomas Jacob
Order of Authors:	Nithin Thomas Jacob Jeroen Lauwaert Bart Vermang Johan Lauwaert
Abstract:	<p>Carbon capture and utilization (CCU) is a promising solution for reducing reliance on fossil fuels and incentivizing the capture of CO₂. A key requirement for CCU is the development of effective photo/electrocatalysts with high CO₂ reduction activity that can produce high-value products. Direct Z-scheme heterojunctions named after their charge transfer mechanism, use sunlight to conduct various photocatalytic reactions, similar to photosynthesis in plants. Solar cell simulation techniques can be used to obtain material properties and insights into the electronic characteristics of these materials. By solving semiconductor differential equations that model the behavior of semiconductors under different light intensities and applied biases, the solar cell simulator program (SCAPS) can evaluate the energy band edges, carrier concentrations, and output characteristics of the device. In this study, a method is proposed for modeling direct Z-scheme junctions in SCAPS by simulating the Shockley Read Hall (SRH) recombination using defect densities at the interface of the recombination junction (RJ). An example using a TiO₂/CdIn₂S₄ Z-scheme junction is presented and the impact of defects on the performance of the junction is discussed. It is presented that the high recombination rates at the interface via these defects improve the device performance.</p>
Suggested Reviewers:	<p>Sakshi Tyagi KU Leuven - Kulak Kortrijk Campus sakshi.tyagi@kuleuven.be</p> <p>Devika Rajagopal KU Leuven devika.rajagopal@imec.be</p> <p>Govind Padmakumar Delft University of Technology Faculty of Electrical Engineering Mathematics and Computer Science G.Padmakumar@tudelft.nl</p> <p>Samira Khelifi Ghent University Faculty of Sciences Samira.Khelifi@UGent.be</p>





Highlights

Numerical device modeling for direct Z-scheme junctions using a solar cell simulator

Nithin Thomas Jacob , Jeroen Lauwaert , Bart Vermang , Johan Lauwaert 

- Usage of solar cell simulators to study semiconductor catalysts is demonstrated.
- Insights on Direct Z-scheme junctions functioning is reported.
- An example using an established Direct Z-scheme junction is shown.
- The influence of various parameters on the junction performance is reported.
- The importance of recombination of charge carriers at the Z-scheme junction interface is reported.

Numerical device modeling for direct Z-scheme junctions using a solar cell simulator

Nithin Thomas Jacob , Jeroen Lauwaert , Bart Vermang , Johan Lauwaert 

^a*Department of Electronics and Information Systems, Ghent University, Technologiepark 126, Zwijnaarde, 9052, Ghent, Belgium*

^b*Department of Materials, Textiles and Chemical Engineering, Ghent University, Valentin Vaerwyckweg 1, Ghent, 9000, Ghent, Belgium*

^c*Institute for Material Research (IMO), Hasselt University, Agoralaan gebouw H, Diepenbeek, B-3590, Diepenbeek, Belgium*

^d*IMEC Division IMOMEC — Partner in Solliance, Wetenschapspark 1, Diepenbeek, B-3590, Diepenbeek, Belgium*





^e*EnergyVille, Thor Park 8320, Genk, B-3600, Genk, Belgium*

^f*Department of Electronics and Information Systems, Ghent University, Technologiepark 126, Zwijnaarde, 9052, Ghent, Belgium*

Abstract

Carbon capture and utilization (CCU) is a promising solution for reducing reliance on fossil fuels and incentivizing the capture of CO₂. A key requirement for CCU is the development of effective photo/electrocatalysts with high CO₂ reduction activity that can produce high-value products. Direct Z-scheme heterojunctions named after their charge transfer mechanism, use sunlight to conduct various photocatalytic reactions, similar to photosynthesis in plants. Solar cell simulation techniques can be used to obtain material properties and insights into the electronic characteristics of these materials. By solving semiconductor differential equations that model the behavior of semiconductors under different light intensities and applied biases, the solar cell simulator program (SCAPS) can evaluate the energy band edges, carrier concentrations, and output characteristics of the device. In this study, a method is proposed for modeling direct Z-scheme junctions in SCAPS by simulating the Shockley Read Hall (SRH) recombination using defect densities at the interface of the recombination junction (RJ). An example using a TiO₂/CdIn₂S₄ Z-scheme junction is presented and the impact of defects on the performance of the junction is discussed. It is presented that the high recombination rates at the interface via these defects improve the device performance.

Keywords: Semiconductor, Catalysis, Simulations, Modelling, Photocatalysis, Electrocatalysis

Email addresses: nithintj101@outlook.com (Nithin Thomas Jacob )
Jeroen.Lauwaert@UGent.be (Jeroen Lauwaert )
Bart.Vermang@imec.be (Bart Vermang )
Johan.Lauwaert@UGent.be (Johan Lauwaert )

1. Introduction

Due to the enormous emissions of greenhouse gases such as CO₂ which trap heat on earth and insulate it from the cold of space, the threat of climate change is imminent.

To reduce the CO₂ emissions, various Carbon Capture and Utilization (CCU) technologies have been emerging. [1]. In CCU, the captured CO₂ is reduced into products such as methanol that can be used in transportation fuels [2]. This promotes a carbon neutral economy by chemical reduction of captured CO₂ from the atmosphere to value products using renewable energy sources and decreasing reliance on fossil fuels for their production.

The reduction of CO₂ is thermodynamically and kinetically challenging as it consists of the breaking of two C=O bonds that have a bond dissociation energy of 750 kJ/mol [3]. Catalysts can facilitate these reactions to synthesize high-value products such as dimethyl ether (DME), olefins and higher alcohols without relying on conventional energy sources [4].

Semiconductor catalysts are good candidates for this application. It has been reported that homogeneous catalysts for electro-, photo- and photoelectrocatalytic CO₂ reduction reactions offer higher activities and selectivities than heterogeneous counterparts. However, the former is quite difficult to separate from the reaction mixture, thereby making them unsuitable for re-use, which is disadvantageous in terms of sustainability [3].

1.1. Semiconductor Catalysis

In 1972, Fujishima and Honda reported that the semiconductor TiO₂ can be used as a photocatalyst in water to produce Hydrogen [5]. This led to extensive research and development in the area of semiconductor catalysts to improve their photocatalytic efficiency and deployment in various applications especially in the sustainability sector [6].

These catalysts are used in various applications. It is reported that the material has usage in applications such as wastewater treatment [7, 8, 9], hydrogen production [10, 11, 12], CO₂ reduction [13, 14, 15, 16] and air purification [17, 18, 19]. There are various ways in which an established photocatalyst can be improved using dye anchoring, metal deposition, heterogeneous composites, doping, surface adsorbates and hybrids with nano-materials [6].

Although TiO₂ can facilitate water splitting into H₂ and O₂, its large bandgap of 3.2 eV allows it to utilize the UV part of the spectrum, which results in a low spectral utilization. Hence, novel semiconductor materials with lower band gap and efficient charge separation need to be explored as candidates to improve this spectral utilization [20].



In Equation 1, we take the case of a redox reaction of reactant "O" and product "R" at potential V_{redox}° (in volts against the normal hydrogen electrode

Rev #1
Comment 1.a.

(NHE)). This can be measured in terms of energy levels E_{redox} (denoted in electron volts against vacuum) using the relationship as:

$$E_{redox} = constant - eV_{redox}^{\circ} \quad (2)$$

Where the *constant* value is between -4.48 eV and e is the unit charge [21].

The semiconductor catalyst must supply charge carriers that are (i) electrons, at a higher energy level than their reduction level and (ii) holes are supplied lower than the reaction oxidation energy level. Moreover, extra energy is needed to overcome the reaction overpotentials. Hence, using these semiconductor catalysts we can conduct reactions in a non-spontaneous direction by adding irradiant energy and/or electrical energy that can be converted to chemical energy as fuel [21]. This is ideal for the current demand for emission free production methods of chemical synthesis.

1.2. Direct Z-scheme semiconductors

Z-scheme junctions are composite semiconductors that use a two-photon excitation method to achieve higher charge separation similar to photosynthesis in plants. It addresses the issue with single component catalysts like TiO_2 which requires a large bandgap for high charge separation but at the expense of low spectral utilization. These features are mutually exclusive and Z-scheme junctions can in principle overcome this. However, further studies must be carried out to improve their stability, light harvesting, charge separation and transportation to reach economic viability and physical/chemical understanding [22].

Direct Z-scheme semiconductor materials or photosystem (PS-PS) systems are composite semiconductors. This structure is intended to be similar to a tandem solar cell which utilizes junctions of semiconductor materials of different energy band gaps and electron affinities to enhance the solar cell's spectral utilization and produce high voltage outputs i.e. better charge separation. However, in this report, the working of a dual n-type Z-scheme junction is elaborated and is quite different from that of a tandem solar cell.

This paper demonstrates the use of solar cell simulators to model the effectiveness of charge carrier separation in a photocatalyst. The charge carriers are used in the reduction and oxidation sites of the semiconductor catalyst while in a traditional solar cell these carriers contribute directly to electric power generation. Consequently solving the semiconductor equations to describe the carrier kinetics in both systems is equivalent. Moreover, the performance parameters of the photocatalyst as a solar cell will reveal the expectations of the structure under different bias and illumination conditions. This study proposes the use of solar cell simulator SCAPS to simulate direct Z-scheme junctions. For such a Z-scheme heterojunction direct recombination at the interface from both sides needs to be included [23].

It is crucial to engineer photocatalysts that can prevent bulk charge recombination and as such improve the light-harvesting efficiency of the system. Equivalent to thin-film photovoltaic technology, many options to improve water

Rev #1
Comment 1.b.

splitting and CO₂ reduction catalysts have been proposed: bandgap engineering, crystal facet engineering and surface heterojunction optimization [24].

Although characterization of Z-scheme junctions using experimental methods such as photo reduction testing, radical species trapping, metal loading and X-ray photoelectron spectroscopy (XPS) are present [25]. These techniques do not establish a direct link between the experimental parameters and the final device efficiency of converting irradiation to chemical energy. Simulations can address these issues by using the experimental data from characterization and estimating the impact on efficiency by evaluating the charge carrier migration in the photo-catalyst [25].

In this paper, a method to solve the semiconductor equations for a Z-scheme heterojunction is presented. This is done by including defect traps at the interface to allow the photo-generated low energy carriers to recombine, thereby achieving high open circuit voltage (V_{OC}) or charge separation compared to the oxidation or reduction potentials of the desired product.

1.3. Solar Cell Capacitance Simulator (SCAPS)

Solar cell capacitance simulator (SCAPS 1-D) was developed at Ghent University and is available for the research community [26]. It is used to simulate the performance of thin film solar cells and can simulate conventional characterization techniques. The program was developed initially for structures such as CuInSe₂ and CdTe cells, but due to the generality of the semiconductor equations that are solved other structures can be modeled.

The simulator has user-friendly and a graphical interface that gives output data that is useful for the catalyst research and development community. A key reason why SCAPS is used over other solar simulators is because of its ability to include a recombination model based on defects with different properties that are desired in the working of this model and is elaborated further in Section 2.2.

2. Methodology

The primary objective of this study is to evaluate the direct Z-scheme device performance. This is indicated by the efficient conversion of sunlight to electric power or charge carriers that can be used for redox reactions. The three main solar cell parameters used to describe the desired characteristics are:

- the efficiency (η) to indicate the effective conversion of sunlight to generated power.
- current density at maximum power point (J_{MPP}) to indicate the number of carriers to oxidation and reduction sites in the Z-scheme catalyst.
- the voltage at maximum power point (V_{MPP}) is induced potential that indicates whether the reduction and oxidation potentials for the concerning reaction can be exceeded. Higher charge separation is preferred to overcome any overpotentials.

Rev #1

Comment 1.c.

The characteristics and requirements of the catalytic device are similar to those of a solar cell device. This makes solar simulators a viable tool to study the photo, electro or photo electro-catalytic semiconductors.

An established direct Z-scheme junction $\text{TiO}_2/\text{CdIn}_2\text{S}_4$ that is used to reduce and oxidize methyl orange (MO) is used as reference material [27]. It is reported that methyl orange redox potentials are -0.33/2.40 eV (vs. NHE) [27]. The candidate Z-scheme junction should supply a V_{MPP} greater than the difference between the redox potential difference. An overpotential must be added into the redox potential difference for example 0.5 V when using TiO_2 passivated GaP photocatalysts [28]. However, for a prima facie analysis, this is not required and hence omitted in this study.

The (conduction band quasi fermi level) E_{F_N} at the reduction site must be higher than the reduction potential of the reaction and the (valence band quasi fermi level) E_{F_P} at the oxidation site must be lower than the oxidation reaction. This will help in evaluating the feasibility of charge carriers to move from the semiconductor material and take part in the chemical reaction. This is similar to the metalwork function of a contact in a solar cell and electron or hole transport layer. It is reported that the TiO_2 and CdIn_2S_4 have E_{CB}/E_{VB} levels at -0.29/2.91 eV and -0.82/1.38 eV (vs. NHE) which are the material parameters implemented in SCAPS as input parameters [27]. Since the energy levels meet the primary criteria, they can be considered good candidates for a Z-scheme junction for methyl orange oxidation and reduction catalysis.

Bard et al. state that the properties of the electrolyte can also be modeled as an intrinsic semiconductor with specific parameters [21]. Such an approximation is not experimentally validated in combination with a Z-scheme, therefore this is not included in our proposed model in this paper. This can be proposed as future work. This paper will focus on modeling the Z-scheme junction.

2.1. Numerical modeling of semiconductor devices

Partial differential equations are used to model the behavior of charge carriers in semiconductor devices [29].

Poisson's equation in the one-dimensional case is written as:

$$\frac{d^2\psi}{dx^2} = \frac{dE}{dx} = -\frac{q}{\epsilon}[N(x) + p - n] \quad (3)$$

Where ψ stands for the potential, E stands for the electric field, x for the position, $N(x)$ is the net charge concentration of the impurities or dopants, q is the electronic charge, ϵ is the dielectric constant of the semiconductor layer, p and n are the hole and electron densities, respectively. The charge carrier concentration in the semiconductor is evaluated using the continuity equations at steady state conditions across the cell thickness as:

$$\begin{aligned} \frac{1}{q} \frac{dJ_n}{dx} &= U - G \\ \frac{1}{q} \frac{dJ_p}{dx} &= -(U - G) \end{aligned} \quad (4)$$

Table 1: Semiconductor layer parameters used in this study.

	PS I	PS II
Material	TiO ₂	CdIn ₂ S ₄
Thickness [μm]	2	2
Bandgap [eV]	3.2	2.2
Electron affinity [eV]	5.81	4.78
Dielectric permittivity	10	10
CB effective density of states [$10^{19} \text{ cm}^3/\text{s}$]	1	1
VB effective density of states [$10^{19} \text{ cm}^3/\text{s}$]	1	1
Electron thermal velocity [10^7 cm/s]	1	1
Hole thermal velocity [10^7 cm/s]	1	1
Electron mobility [$\text{cm}^2/\text{V s}$]	50	50
Hole mobility [$\text{cm}^2/\text{V s}$]	50	50
Shallow uniform donor density (N_D) [10^{12} 1/cm^3]	1	9000
Shallow uniform acceptor density (N_A) [$1/\text{cm}^3$]	10	10
Radiative recombination coefficient [$10^{-4} \text{ cm}^3/\text{s}$]	1	1

Table 2: Interface layer parameters used in this study are assumed. σ is capture cross-section.

Parameter type	Value
Defect type	Neutral
σ_e [10^{-19} cm^2]	1
σ_h [10^{-19} cm^2]	1
Energetic distribution	Single
Reference for defect energy level (E_t)	Above middle of interface gap
Energy with respect to Reference [eV]	0
Total density [10^{10} 1/cm^2]	1

Where J_n and J_p represent the current densities by electrons and holes, respectively. U and G are the recombination and generation rates, respectively [30].

In Table 1, the semiconductor parameters are shown in this model to study the Z-scheme device [27]. In Table 2, the interface properties were given.

The left and right contacts are simulated to have flat bands with electron and hole surface recombination rates of 10^5 and 10^7 cm/s respectively.

2.2. Shockley Read Hall (SRH) recombination at the interface

It is assumed that the low-energy charge carrier recombination at the interface between the layers of the Z-scheme semiconductor is due to the presence of high defect densities. In SCAPS, the proposed recombination can be modeled in the form of SRH recombination at a particular energy state. It is reported that the recombination at these interface defects can be modeled using SRH recombination. This type of recombination path was introduced in SCAPS to

model polycrystalline solar cells such as the interface between CdS/CdTe cells [26].

Many solar cell simulators only treat SRH recombination within the same layer and require a dummy layer in between to handle this. This SRH recombination path from both sides of the interface will be utilized in the Z-scheme model for which low energy carriers from both materials can directly recombine via the interface states.

2.3. Energy band diagram of the Z-scheme heterojunction

Z-scheme junctions require a particular characteristic in their energy band diagram.

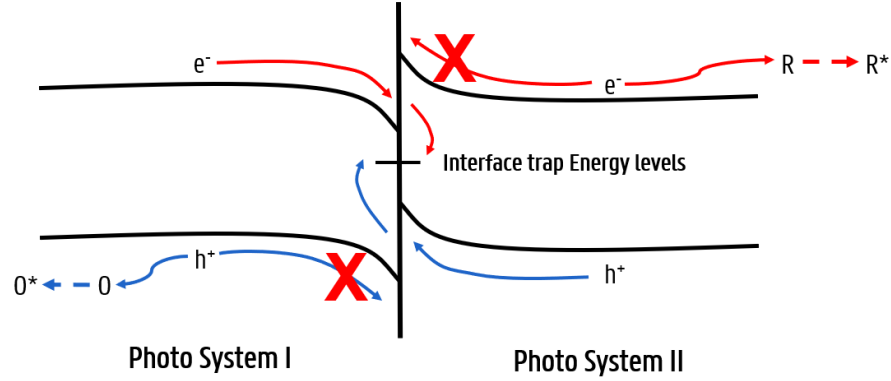


Figure 1: A schematic in the charge carrier propagation in a direct Z-scheme junction. The red line indicates the motion of electrons (e^-) and the blue line indicates the motion of holes (h^+).

Figure 1 illustrates that the valence band in Photosystem I (PS I) layer is required to hold the high energy holes generated to be utilized in the oxidation site, hence an energy barrier must be present. The high energy holes are moved to the oxidation sites where the oxidation reactant O gives an electron to the semiconductor catalyst, forming the oxidized product O^* . The conduction band in Photosystem II (PS II) layer is required to hold the high energy electrons generated to be utilized in the reduction site, hence an energy barrier must be present. The high energy electrons are moved to the reduction sites where the reduction reactant R takes an electron from the semiconductor catalyst, forming the oxidized product R^* . The low energy charge carriers of PS I and PS II are electrons and holes, respectively. They recombine due to the interface states present. This is illustrated in the presence of the valence band and conduction band energy dips.

In the case of the $TiO_2/CdIn_2S_4$ Z-scheme junction which is modeled in this study. The illumination of AM1.5 1 sun spectrum is falling on the TiO_2 layer first. TiO_2 layer is PS I and the $CdIn_2S_4$ layer is PS II in this study.

The recombination at the interface is modeled in SCAPS using defects at trap energy levels between the PS I and PS II conduction and valence band edges.

A direct Z-scheme heterojunction model is developed to resemble the working of a Z-scheme junction in a solar cell simulator such as SCAPS. The recombination of low energy charge carriers is simulated using SRH recombination of these carriers in neutral defects in the interface between the two semiconductor layers.

2.4. Model validation

Open circuit voltage or V_{OC} of the semiconductor device is the direct measurement of the charge separation capability. The reduction and oxidation capability of the catalyst is proportional to the V_{OC} . The short circuit current or J_{SC} of the semiconductor is an important characteristic to note as well, as it quantifies the amount of high energy charge carriers that are available at the reduction and oxidation sites. The efficiency translates to the utilization of solar irradiation by the material.

To evaluate whether the modeled structure is a Z-scheme junction the current that should be matched in both photosystems should cross the interface via recombination. In such a situation, the ideal case is when low-energy charge carriers recombine at the interface and the high-energy charge carriers exit the device into the contacts, where they can be used for reduction and oxidation.

3. Results and Discussion

SCAPS models the Z-scheme junction at a given irradiation and gives the corresponding current density-voltage (JV) curve. The solar cell parameters are estimated using this JV curve. The energy bands can be simulated at a given voltage. It is useful in establishing whether the junction modeled is indeed a Z-scheme junction.

3.1. Energy band diagram

The energy band diagram of the modeled Z-scheme junction is given in Figure 2. The charge carriers must be at the energy levels that are required for the redox reactions to occur. It must be noted that a Z-scheme junction also has a distinct energy band diagram with barriers at the interface to facilitate the recombination of low-energy carriers and to hold the high-energy carriers to be supplied to the respective reaction sites [13].

Figure 2 illustrates the energy band diagram of the $TiO_2/CdIn_2S_4$ with respect to the fermi level (E_F) of neutral TiO_2 . On the left side of the device, we have the TiO_2 layer with its distinctive high energy gap and higher electron affinity. On the right side, we have the $CdIn_2S_4$ layer with a lower energy gap and lower electron affinity.

It is noted that the band bending generated in the simulated materials is that of the direct Z-scheme as the energy barriers in the PS II ($CdIn_2S_4$ layer) conduction band keeps the electrons at high energy and can be used in the

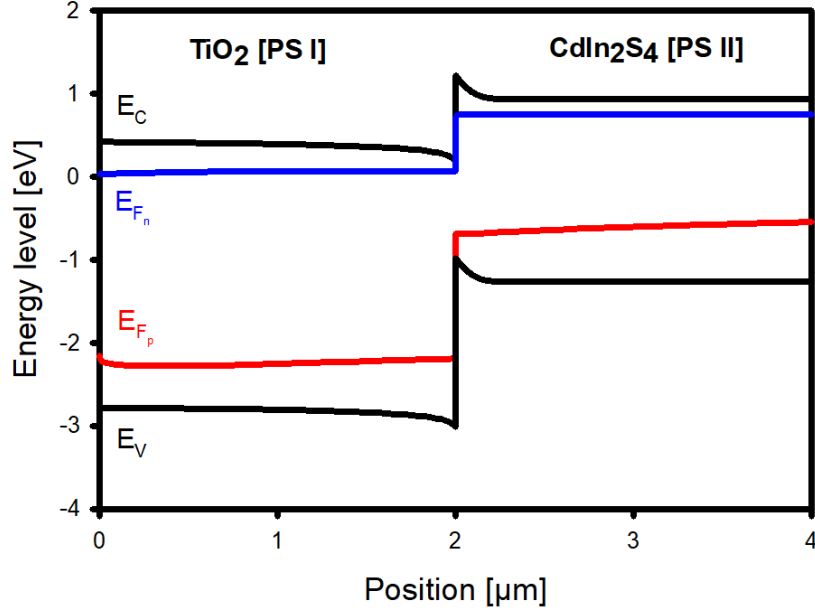


Figure 2: Energy band diagram of the $\text{TiO}_2/\text{CdIn}_2\text{S}_4$ Z-scheme junction in SCAPS with respect to the fermi level E_F of neutral TiO_2 (0.4175 eV wrt. vacuum) at the illumination of 1000 W/m^2 and 0 V.

reduction sites. The same can be concluded for the valence band of PS I (TiO_2 layer) for holes that can be supplied to the oxidation sites. This confirms that the established $\text{TiO}_2/\text{CdIn}_2\text{S}_4$ Z-scheme junction shows the modeled energy band diagram which is desired for a Z-scheme junction.

Figure 3 illustrates the calculated charge carrier concentration in the modeled Z-scheme device. The specific band offset results in an increased concentration of electrons and holes close to the interface ($x = 2 \mu\text{m}$). The high charge concentrations facilitate a high recombination rate for electrons in PS I and holes in PS II.

The recombination at the interface is signified by the high peaks and troughs formed at the interface between the PS I and PS II layers of the Z-scheme junction at the interface at $2 \mu\text{m}$ (total thickness $4 \mu\text{m}$). For equivalent capture cross-sections of the interface defects, the capture rate is proportional to the carrier concentration at the interface and thus capture of electrons from PS I and holes from PS II will be the most important terms in the SRH mechanism. Defects are present at the trap energy level between the conduction band of TiO_2 and the valence band of CdIn_2S_4 . The low-energy charge carriers shall meet up at these defect sites and undergo SRH recombination.

SCAPS then simulates the JV curve of the device and calculates the device

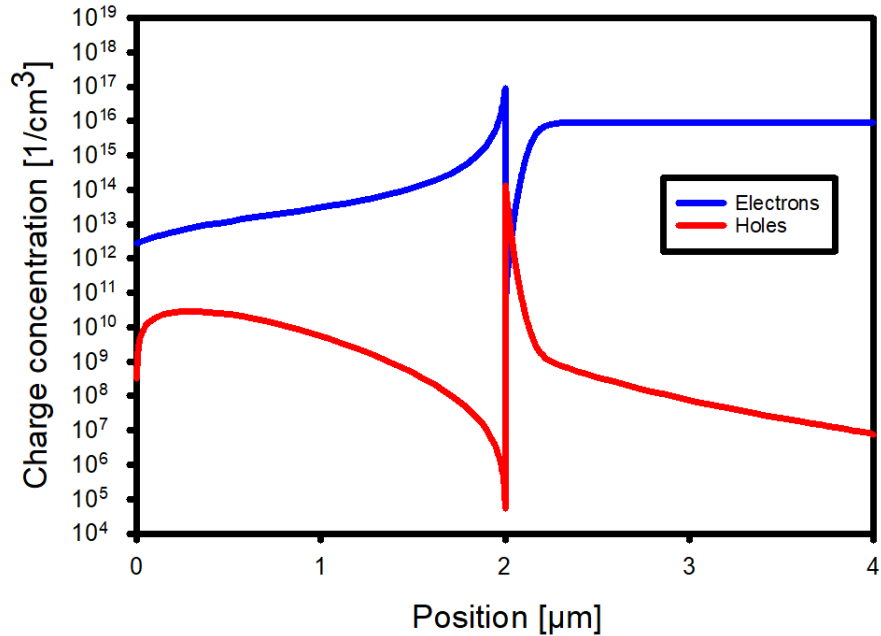


Figure 3: Hole and electron concentration across the modeled Z-scheme device thickness in red and blue line, respectively from SCAPS model at 1000 W/m^2 and 0 V .

performance parameters as in Figure 4. In this case, the corresponding solar cell parameters are shown in Table 3. It can be seen that the JV curve of this modeled Z-scheme device is unlike an efficient solar cell Z-scheme curve where the open circuit voltage is made to work very close to the maximum power point. This can be attributed to the low fill factor (FF) of the heterojunction. FF is defined as the ratio between the maximum power density of the device which is the green area and the product of V_{OC} and J_{SC} which is the grey area in Figure 4.

The low fill factor compared to that observed in solar cells is because unlike in solar cells where the objective is to collect maximum number of charge carriers at contacts for electrical power generation. The objective of a direct Z-scheme device used in catalysis would be maximum charge separation. This would be possible with the low energy charge carriers recombining and thereby utilizing high energy charge carriers for power generation or reduction/oxidation catalysis.

3.2. Defect density effect

The defect densities at the interface play an important role in the model as they provide the recombination levels for the recombination junction in between

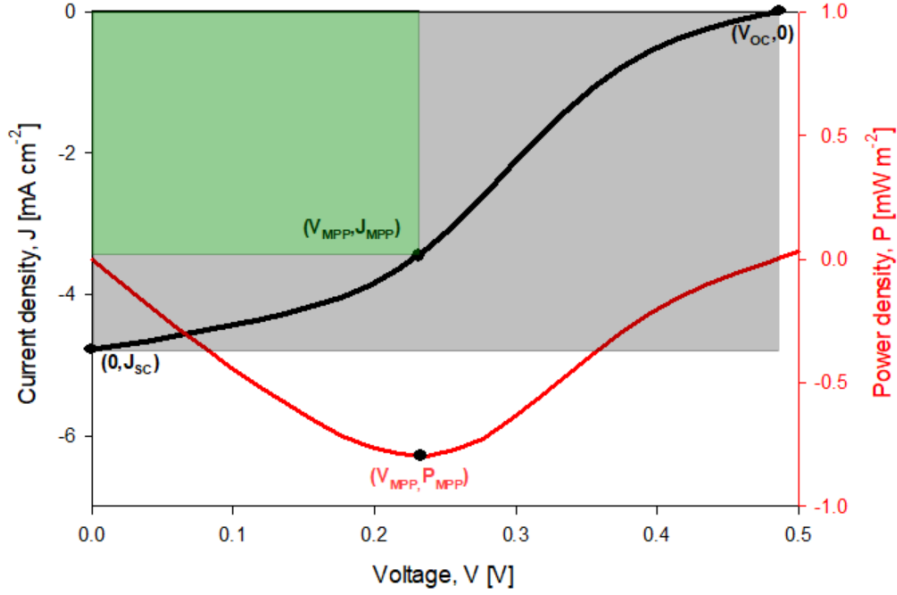


Figure 4: SCAPS current density vs. voltage characteristics (JV curve) in black and Power density vs. voltage in red on applying AM1.5 solar spectrum on $\text{TiO}_2/\text{CdIn}_2\text{S}_4$ Z-scheme junction. With illumination on the right side (TiO_2 side). The grey area indicates $V_{\text{OC}} \times J_{\text{SC}}$ and the green area is $V_{\text{MPP}} \times J_{\text{MPP}}$ which is P_{MPP} ie., maximum power density.

the photosystems for the device which is the interface. By increasing the density of these trap defects, there are more sites for the low energy charge carriers to occupy for recombination as illustrated in Figure 1. This will allow the high energy charge carriers to be separated and utilized for reduction and oxidation reactions. It is investigated if the type of defect (neutral, acceptor or donor) has a role in the cell performance as well. Figure 5 illustrates that there is a direct correlation between the total defect density at the interface and the performance of the solar cell parameters. As the total defect density is increased, there is an increase in all cell parameters as cell efficiency (η), V_{OC} , J_{SC} and FF.

A key takeaway here is that the number of recombination sites increases at the interface, the cell parameters of the Z-scheme junction improves with better charge separation and better charge density at the oxidation and reduction sites.

The effect of the type of defect is shown above in Figure 6. The acceptor or donor nature of the defect type was found to have no profound effect on the model characteristics as the cell parameters showed little to no variation. There is consistent overlapping of the Z-scheme JV curves for different defect types. This indicates that the charge of the interface defects has a negligible impact on the interface recombination rate and efficiency of the device as well.

Table 3: SCAPS device parameters of the simulated $\text{TiO}_2/\text{CdIn}_2\text{S}_4$ Z-scheme junction from the JV curve in Figure 4.

Parameters	Unit	Value
Open circuit voltage, V_{OC}	[mV]	480
Short circuit current, J_{SC}	[mA/cm ²]	4.78
Fill factor, FF	[%]	34.32
Efficiency, η	[%]	0.79
Voltage at maximum power point, V_{MPP}	[V]	0.23
Current at maximum power point, J_{MPP}	[mA/cm ²]	3.44

Rev #1
Comment 1.d.

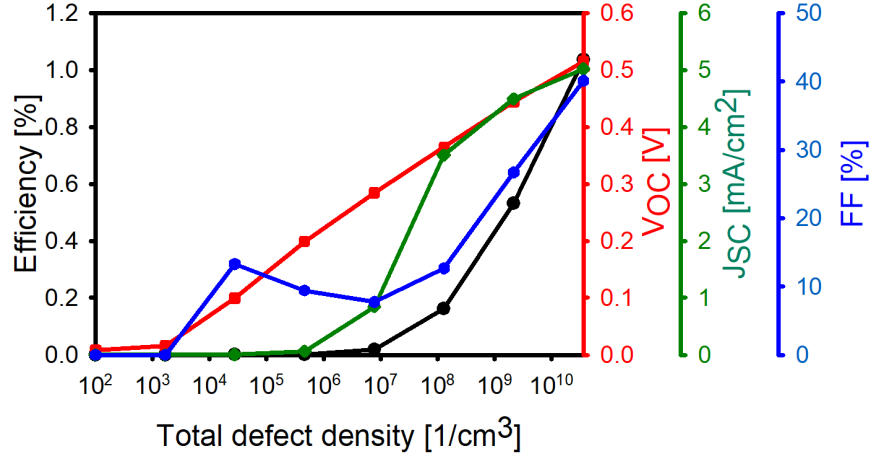


Figure 5: Solar cell parameters plotted as a function of the total defect density at the interface from SCAPS. The cell efficiency (η) is indicated in black, the open circuit voltage (V_{OC}) is indicated in red, the short circuit current (J_{SC}) is indicated in green and the fill factor (FF) is indicated in blue.

3.3. Band offsets effect

In the previous section, it is shown that the recombination at the interface has a direct correlation with the **performance of the device**. One can study the influence of the energy barriers and dips can have on the Z-scheme device using solar simulators. It is noted that these barriers help in isolating the high-energy charge carriers from the low-energy charge carriers. The dips in the energy band diagram in Figure 2 will help the recombination of the low-energy charge carriers. To study the influence of these band offsets, the PS I remained constant the energy position of the band edges of PS II are varied. Two options are described below.

Rev #1
Comment 1.e.

Rev #1
Comment 3

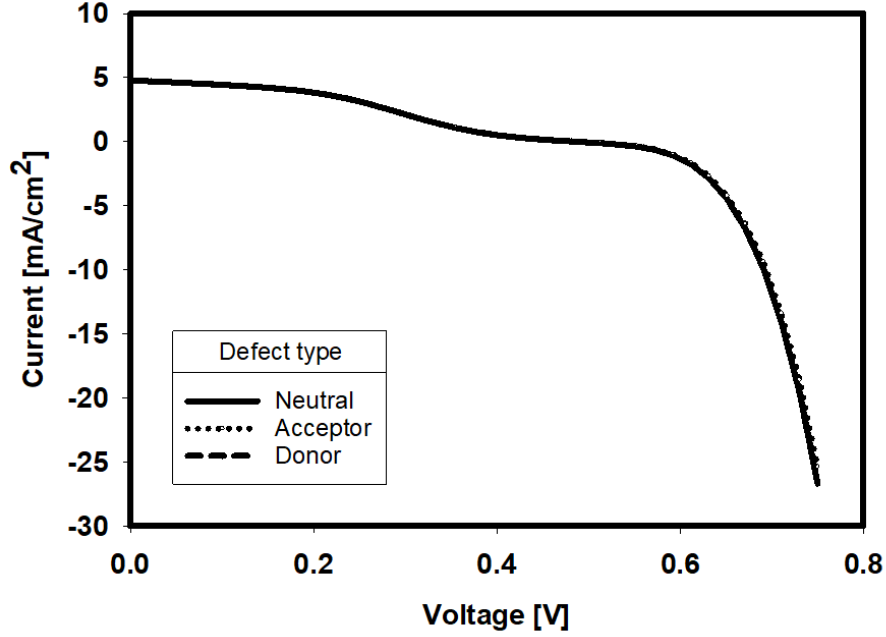


Figure 6: Effect of defect type being "neutral" i.e, a hypothetical center carrying no charge, donor or acceptor on the JV curve of the simulated Z-scheme device from SCAPS.

3.3.1. Fixed PS II conduction band

The conduction band of PS II is fixed at 4.78 eV which is the electron affinity of the CdIn_2S_4 material. The PS II energy gap is varied from 1 eV to 3 eV which changes the valence band position with respect to the conduction band in the model. The solar cell performance parameters as a function of PS II energy gap is shown in Figure 7.

Figure 7 illustrates the effect of the energy gap of PS II on the performance of the Z-scheme junction with fixed PS II conduction band. Device efficiency increases to a maximum of about 1.5% at about 1.1 eV and then decreases as the energy gap is increased. An irregularity in the fill factor (FF) and V_{OC} curve close to 1.5 eV can also be noticed. For these band offsets, convergence failure occurred in SCAPS induced by the high free carrier concentrations at the interface.

The efficiency curve can be explained as it follows the V_{OC} trend initially till the rise to maxima and then the J_{SC} trend during its fall with an increase in the energy gap (E_g) of the photosystem II (PS II) semiconductor layer.

When the bandgap energy (E_g) of PS II is 1 eV, the conduction band edge of PS I with respect to vacuum is at 5.81 eV (electron affinity (X) of PS I) and the valence band of PS II is $X + E_g$ i.e. 5.78 eV. It means that the valence band edge of PS II is above the conduction band edge of PS I by about 0.03 eV.

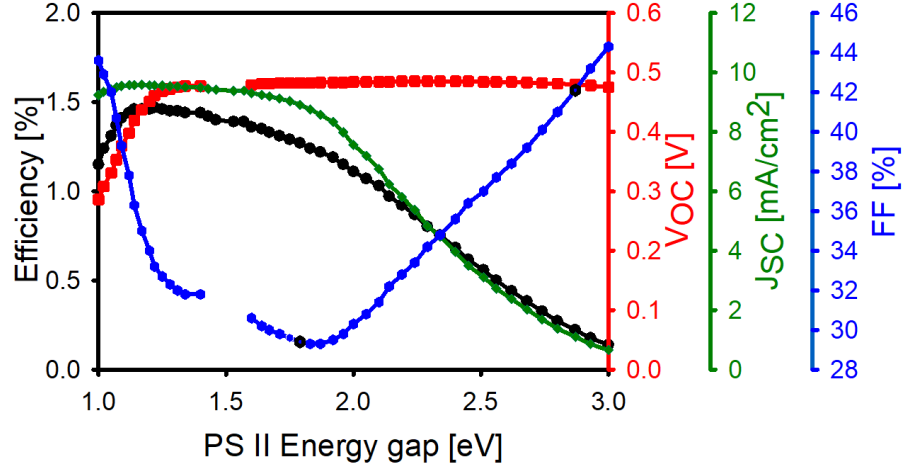


Figure 7: The solar cell parameters as a function of the PS II Energy bang gap from SCAPS model. The cell efficiency (η) is indicated in black, the open circuit voltage (V_{OC}) is indicated in red the short circuit current (J_{SC}) is indicated in green and the fill factor (FF) is indicated in blue. Results obtained from the SCAPS model.

This leads to a structure with no interface band gap with a high concentration of low energy carriers and there will be no interface recombination occurring due to the interface defects. As the E_g of PS II is increased, the interface gap increases. This leads to the defects being utilized for the low energy charge carriers recombination. As the energy gap is increased further, the charge carrier generation is dropped as a lower number of photons is absorbed in the PS II layer due to its large bandgap. The model is able to predict an optimal structure when the energy gap of PS II is 1.1 eV.

3.3.2. Fixed PS II valence band

The valence band is fixed by making sure that the sum of electron affinity and energy gap is constant. The energy position of the valence band corresponds with the values in Table 1. Parameter sweeps are conducted for values of PS II E_a and PS II E_g where the sum stays 6.98 eV. The results of the parameter sweep is shown in the Figure 8 as a function of the PS II energy gap.

As the PS II energy gap is increased from 1.0 to 1.69 eV. The device shows little to no performance as the PS II conduction band is below the conduction band of the PS I. Therefore, there is no barrier for electrons generated and the recombination mechanism at the interface is not the preferential mechanism for carrier collection. As the PS II energy gap is further increased which means the electron affinity of PS II is decreasing. The PS II conduction band continues to move away from the PS I conduction band making a positive band offset in the conduction band from PS I to PS II. This barrier keeps the high energy charge carriers from going to a low energy level and allows the recombination of

Rev #1
Comment 3

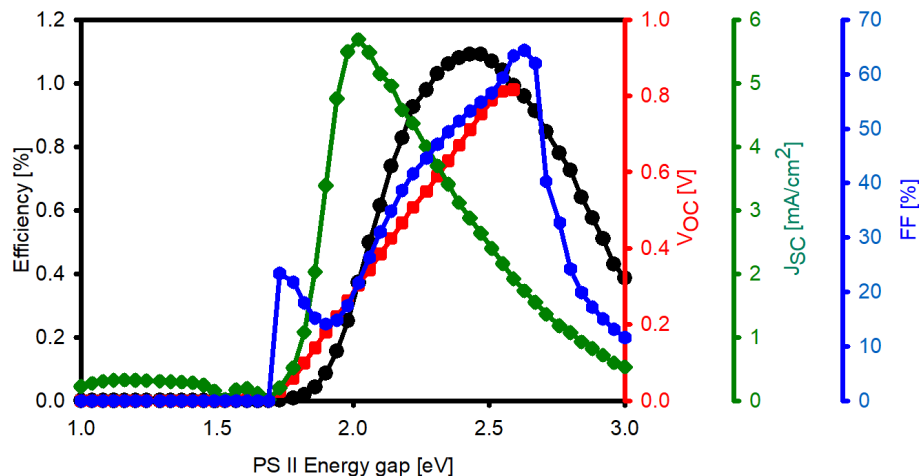


Figure 8: The solar cell parameters as a function of the PS II energy gap from SCAPS model. Where the PS II satisfies the condition that the sum of the energy gap and electron affinity is 6.98 eV. The cell efficiency (η) is indicated in black, the open circuit voltage (V_{OC}) is indicated in red the short circuit current (J_{SC}) is indicated in green and the fill factor (FF) is indicated in blue. Results obtained from the SCAPS model.

low energy charge carriers. On the other hand, when the energy gap is further increased. The generation of carriers in PS II will reduce. Hence, there is a maximum in the device efficiency. The efficiency curve rises to a maxima of 1.09% at PS II energy gap of 2.43 eV. The only performance parameter that gradually rises is the V_{OC} due to the rise in the built-in potential in the junction. The absence of data points beyond 2.6 eV is due to convergence failures occurring in SCAPS when calculating the open circuit potential for these points.

Rev #1
Comment 3

4. Conclusion

Z-scheme semiconductor materials have desirable optoelectrical properties that make them viable chemical catalysts for reduction and oxidation reactions. As there are various combinations of semiconductor layers possible for this composite material, the development of a screening model was imperative to evaluate the feasibility of the material and the desired application. It can be used as a primary study tool to evaluate various semiconductor candidates that can be used for charge carrier generation for chemical reduction and oxidation.

It is concluded that solar cell simulators such as SCAPS are powerful tools to assess Z-scheme junctions. Its user-friendly interface is beneficial in reducing the learning curve for the catalyst research community. The cell parameters can help in giving a prima-face analysis of the feasibility of using certain materials as a catalyst.

The modeling methodology of a direct Z-scheme junction using a solar cell simulator (SCAPS) is presented in this study. The key performance indicators are presented along with an example case using an established junction ($\text{TiO}_2/\text{CdIn}_2\text{S}_4$). A direct correlation between the recombination of low-energy carriers at the interface and device performance is presented.

Data availability

Data will be available from the corresponding author upon reasonable request.

References

- [1] F. D. Meylan, V. Moreau, S. Erkman, [CO₂ utilization in the perspective of industrial ecology, an overview](#), Journal of CO₂ Utilization 12 (2015) 101–108. doi:10.1016/j.jcou.2015.05.003. URL <http://dx.doi.org/10.1016/j.jcou.2015.05.003>
- [2] R. M. Cuéllar-Franca, A. Azapagic, Carbon capture, storage and utilisation technologies: A critical analysis and comparison of their life cycle environmental impacts, Journal of CO₂ Utilization 9 (2015) 82–102. doi:10.1016/j.jcou.2014.12.001.
- [3] Y. Wang, D. He, H. Chen, D. Wang, Catalysts in electro-, photo- and photoelectrocatalytic CO₂ reduction reactions, Journal of Photochemistry and Photobiology C: Photochemistry Reviews 40 (2019) 117–149. doi:10.1016/j.jphotochemrev.2019.02.002.
- [4] R.-P. Ye, J. Ding, W. Gong, M. D. Argyle, Q. Zhong, Y. Wang, C. K. Russell, Z. Xu, A. G. Russell, Q. Li, et al., CO₂ hydrogenation to high-value products via heterogeneous catalysis, Nature communications 10 (1) (2019) 5698.
- [5] A. Fujishima, K. Honda, [Electrochemical photolysis of water at a semiconductor electrode](#), Nature 238 (1972) 37–38. doi:10.1038/238037a0. URL <https://doi.org/10.1038/238037a0>
- [6] F. Zhang, X. Wang, H. Liu, C. Liu, Y. Wan, Y. Long, Z. Cai, Recent advances and applications of semiconductor photocatalytic technology, Applied Sciences (Switzerland) 9 (2019). doi:10.3390/app9122489.
- [7] Y. Horie, D. A. David, M. Taya, S. Tone, [Effects of light intensity and titanium dioxide concentration on photocatalytic sterilization rates of microbial cells](#), Industrial & Engineering Chemistry Research 35 (1996) 3920–3926, doi: 10.1021/ie960051y. doi:10.1021/ie960051y. URL <https://doi.org/10.1021/ie960051y>

- [8] C. Jin, X. Liu, L. Tan, Z. Cui, X. Yang, Y. Zheng, K. W. K. Yeung, P. K. Chu, S. Wu, [Ag/AgBr-loaded mesoporous silica for rapid sterilization and promotion of wound healing](#), *Biomaterials Science* 6 (2018) 1735–1744. doi:10.1039/C8BM00353J. URL <http://dx.doi.org/10.1039/C8BM00353J>
- [9] R. Wang, W. Zhang, W. Zhu, L. Yan, S. Li, K. Chen, N. Hu, Y. Suo, J. Wang, [Enhanced visible-light-driven photocatalytic sterilization of tungsten trioxide by surface-engineering oxygen vacancy and carbon matrix](#), *Chemical Engineering Journal* 348 (2018) 292–300. doi:https://doi.org/10.1016/j.cej.2018.05.010. URL <https://www.sciencedirect.com/science/article/pii/S138589471830799X>
- [10] C. S. Praveen, *Semiconductors as catalysts for water*, Materials Research Laboratory (2012).
- [11] Q. Li, B. Guo, J. Yu, J. Ran, B. Zhang, H. Yan, J. R. Gong, [Highly efficient visible-light-driven photocatalytic hydrogen production of CdS-cluster-decorated graphene nanosheets](#), *Journal of the American Chemical Society* 133 (2011) 10878–10884, doi: 10.1021/ja2025454. doi:10.1021/ja2025454. URL <https://doi.org/10.1021/ja2025454>
- [12] R. Wang, S. Ni, G. Liu, X. Xu, [Hollow CaTiO₃/La/Cr co-doping for efficient photocatalytic hydrogen production](#), *Applied Catalysis B: Environmental* 225 (2018) 139–147. doi:https://doi.org/10.1016/j.apcatb.2017.11.061. URL <https://www.sciencedirect.com/science/article/pii/S092633731731127X>
- [13] L. Chen, Y. Qin, G. Chen, M. Li, L. Cai, Y. Qiu, H. Fan, M. Robert, T.-C. Lau, [A molecular noble metal-free system for efficient visible light-driven reduction of CO₂ to CO](#), *Dalton Transactions* 48 (2019) 9596–9602. doi:10.1039/C9DT00425D. URL <http://dx.doi.org/10.1039/C9DT00425D>
- [14] W. Tan, B. Cao, W. Xiao, M. Zhang, S. Wang, S. Xie, D. Xie, F. Cheng, Q. Guo, P. Liu, [Electrochemical reduction of CO₂ on hollow cubic Cu₂O@Au nanocomposites](#), *Nanoscale Research Letters* 14 (2019) 63. doi:10.1186/s11671-019-2892-3. URL <https://doi.org/10.1186/s11671-019-2892-3>
- [15] D. Vidyasagar, N. Manwar, A. Gupta, S. G. Ghugal, S. S. Umare, R. Boukherroub, [Phenyl-grafted carbon nitride semiconductor for photocatalytic CO₂-reduction and rapid degradation of organic dyes](#), *Catalysis Science & Technology* 9 (2019) 822–832. doi:10.1039/C8CY02220H. URL <http://dx.doi.org/10.1039/C8CY02220H>

- [16] Q. Liu, Y. Zhou, J. Kou, X. Chen, Z. Tian, J. Gao, S. Yan, Z. Zou, [High-yield synthesis of ultralong and ultrathin \$\text{Zn}_2\text{GeO}_4\$ nanoribbons toward improved photocatalytic reduction of \$\text{CO}_2\$ into renewable hydrocarbon fuel](#), Journal of the American Chemical Society 132 (2010) 14385–14387, doi: 10.1021/ja1068596. doi:10.1021/ja1068596. URL <https://doi.org/10.1021/ja1068596>
- [17] Y. Boyjoo, H. Sun, J. Liu, V. K. Pareek, S. Wang, A review on photocatalysis for air treatment: From catalyst development to reactor design, Chemical engineering journal 310 (2017) 537–559.
- [18] X. Fu, W. A. Zeltner, M. A. Anderson, Applications in photocatalytic purification of air, Studies in surface science and catalysis 103 (1997) 445–461.
- [19] A. S. Besov, A. V. Vorontsov, V. N. Parmon, Fast adsorptive and photocatalytic purification of air from acetone and dimethyl methylphosphonate by TiO_2 aerosol, Applied Catalysis B: Environmental 89 (2009) 602–612.
- [20] N. Serpone, A. V. Emeline, Semiconductor photocatalysis - past, present, and future outlook, Journal of Physical Chemistry Letters 3 (2012) 673–677. doi:10.1021/jz300071j.
- [21] A. J. Bard, Photoelectrochemistry and heterogeneous photo-catalysis at semiconductors, Journal of Photochemistry 10 (1979) 59–75. doi:10.1016/0047-2670(79)80037-4.
- [22] P. Zhou, J. Yu, M. Jaroniec, All-solid-state z-scheme photocatalytic systems, Advanced Materials 26 (2014) 4920–4935. doi:10.1002/adma.201400288.
- [23] H. Pauwels, G. Vanhoutte, The influence of interface state and energy barriers on the efficiency of heterojunction solar cells, Journal of Physics D: Applied Physics 11 (5) (1978) 649.
- [24] D. Huang, S. Chen, G. Zeng, X. Gong, C. Zhou, M. Cheng, W. Xue, X. Yan, J. Li, [Artificial z-scheme photocatalytic system: What have been done and where to go?](#), Coordination Chemistry Reviews 385 (2019) 44–80. doi:10.1016/j.ccr.2018.12.013. URL <https://doi.org/10.1016/j.ccr.2018.12.013>
- [25] J. Low, C. Jiang, B. Cheng, S. Wageh, A. A. Al-Ghamdi, J. Yu, A review of direct z-scheme photocatalysts, Small Methods 1 (2017) 1–21. doi: 10.1002/smtd.201700080.
- [26] M. Burgelman, P. Nollet, S. Degraeve, [Modelling polycrystalline semiconductor solar cells](#), Thin Solid Films 361-362 (2000) 527–532. doi: 10.1016/S0040-6090(99)00825-1. URL <https://scaps.elis.ugent.be/>

- [27] Y. Chen, Q. Hu, M. Yu, X. Gong, S. Li, S. Wang, H. Yu, Z. Li, In-situ construction of a direct z-scheme $\text{CdIn}_2\text{S}_4/\text{TiO}_2$ heterojunction for improving photocatalytic properties, *CrystEngComm* 23 (2021) 5070–5077. [doi:10.1039/D1CE00338K](https://doi.org/10.1039/D1CE00338K).
- [28] G. Zeng, J. Qiu, Z. Li, P. Pavaskar, S. B. Cronin, CO_2 reduction to methanol on TiO_2 -passivated GaP photocatalysts, *ACS Catalysis* 4 (10) (2014) 3512–3516.
- [29] W. Shockley, *Electrons and holes in semiconductors: with applications to transistor electronics*, van Nostrand, 1959.
- [30] P. A. Basore, Numerical modeling of textured silicon solar cells using pc-1d, *IEEE Transactions on Electron Devices* 37 (1990) 337–343. [doi:10.1109/16.46362](https://doi.org/10.1109/16.46362).

Acknowledgments

The authors would like to acknowledge Catalisti for their funding through the Moonshot SYN-CAT project. The funder played no role in the study design, data collection, analysis and interpretation of data, or the writing of this manuscript. The cooperation of the consortium partners is acknowledged and appreciated.

Author contributions

JoL conceived the original idea. NTJ and JoL developed and modeled the Z-scheme junction. They were the major contributors to the writing of the manuscript. BV, JoL and JeL provided expert insights and were involved in the proofreading of the manuscript. BV and JoL secured funding for this project. All authors read and approved the final manuscript.

Competing interests

The authors declare no competing financial or non-financial interests.

Additional information

Correspondence and requests for materials should be addressed to Nithin Thomas Jacob and Johan Lauwaert.

Highlights



Numerical device modeling for direct Z-scheme junctions using a solar cell simulator

Nithin Thomas Jacob , Jeroen Lauwaert , Bart Vermang , Johan Lauwaert 

- Usage of solar cell simulators to study semiconductor catalysts is demonstrated.
- Insights on Direct Z-scheme junctions functioning is reported.
- An example using an established Direct Z-scheme junction is shown.
- The influence of various parameters on the junction performance is reported.
- The importance of recombination of charge carriers at the Z-scheme junction interface is reported.





Highlights

Numerical device modeling for direct Z-scheme junctions using a solar cell simulator

Nithin Thomas Jacob , Jeroen Lauwaert , Bart Vermang , Johan Lauwaert 

- Usage of solar cell simulators to study semiconductor catalysts is demonstrated.
- Insights on Direct Z-scheme junctions functioning is reported.
- An example using an established Direct Z-scheme junction is shown.
- The influence of various parameters on the junction performance is reported.
- The importance of recombination of charge carriers at the Z-scheme junction interface is reported.

Numerical device modeling for direct Z-scheme junctions using a solar cell simulator

Nithin Thomas Jacob , Jeroen Lauwaert , Bart Vermang , Johan Lauwaert 

^a*Department of Electronics and Information Systems, Ghent University, Technologiepark 126, Zwijnaarde, 9052, Ghent, Belgium*

^b*Department of Materials, Textiles and Chemical Engineering, Ghent University, Valentin Vaerwyckweg 1, Ghent, 9000, Ghent, Belgium*

^c*Institute for Material Research (IMO), Hasselt University, Agoralaan gebouw H, Diepenbeek, B-3590, Diepenbeek, Belgium*

^d*IMEC Division IMOMEC — Partner in Solliance, Wetenschapspark 1, Diepenbeek, B-3590, Diepenbeek, Belgium*





^e*EnergyVille, Thor Park 8320, Genk, B-3600, Genk, Belgium*

^f*Department of Electronics and Information Systems, Ghent University, Technologiepark 126, Zwijnaarde, 9052, Ghent, Belgium*

Abstract

Carbon capture and utilization (CCU) is a promising solution for reducing reliance on fossil fuels and incentivizing the capture of CO₂. A key requirement for CCU is the development of effective photo/electrocatalysts with high CO₂ reduction activity that can produce high-value products. Direct Z-scheme heterojunctions named after their charge transfer mechanism, use sunlight to conduct various photocatalytic reactions, similar to photosynthesis in plants. Solar cell simulation techniques can be used to obtain material properties and insights into the electronic characteristics of these materials. By solving semiconductor differential equations that model the behavior of semiconductors under different light intensities and applied biases, the solar cell simulator program (SCAPS) can evaluate the energy band edges, carrier concentrations, and output characteristics of the device. In this study, a method is proposed for modeling direct Z-scheme junctions in SCAPS by simulating the Shockley Read Hall (SRH) recombination using defect densities at the interface of the recombination junction (RJ). An example using a TiO₂/CdIn₂S₄ Z-scheme junction is presented and the impact of defects on the performance of the junction is discussed. It is presented that the high recombination rates at the interface via these defects improve the device performance.

Keywords: Semiconductor, Catalysis, Simulations, Modelling, Photocatalysis, Electrocatalysis

Email addresses: `nithintj101@outlook.com` (Nithin Thomas Jacob )
`Jeroen.Lauwaert@UGent.be` (Jeroen Lauwaert )
`Bart.Vermang@imec.be` (Bart Vermang )
`Johan.Lauwaert@UGent.be` (Johan Lauwaert )

1. Introduction

Due to the enormous emissions of greenhouse gases such as CO₂ which trap heat on earth and insulate it from the cold of space, the threat of climate change is imminent.

To reduce the CO₂ emissions, various Carbon Capture and Utilization (CCU) technologies have been emerging. [1]. In CCU, the captured CO₂ is reduced into products such as methanol that can be used in transportation fuels [2]. This promotes a carbon neutral economy by chemical reduction of captured CO₂ from the atmosphere to value products using renewable energy sources and decreasing reliance on fossil fuels for their production.

The reduction of CO₂ is thermodynamically and kinetically challenging as it consists of the breaking of two C=O bonds that have a bond dissociation energy of 750 kJ/mol [3]. Catalysts can facilitate these reactions to synthesize high-value products such as dimethyl ether (DME), olefins and higher alcohols without relying on conventional energy sources [4].

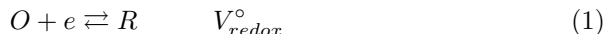
Semiconductor catalysts are good candidates for this application. It has been reported that homogeneous catalysts for electro-, photo- and photoelectrocatalytic CO₂ reduction reactions offer higher activities and selectivities than heterogeneous counterparts. However, the former is quite difficult to separate from the reaction mixture, thereby making them unsuitable for re-use, which is disadvantageous in terms of sustainability [3].

1.1. Semiconductor Catalysis

In 1972, Fujishima and Honda reported that the semiconductor TiO₂ can be used as a photocatalyst in water to produce Hydrogen [5]. This led to extensive research and development in the area of semiconductor catalysts to improve their photocatalytic efficiency and deployment in various applications especially in the sustainability sector [6].

These catalysts are used in various applications. It is reported that the material has usage in applications such as wastewater treatment [7, 8, 9], hydrogen production [10, 11, 12], CO₂ reduction [13, 14, 15, 16] and air purification [17, 18, 19]. There are various ways in which an established photocatalyst can be improved using dye anchoring, metal deposition, heterogeneous composites, doping, surface adsorbates and hybrids with nano-materials [6].

Although TiO₂ can facilitate water splitting into H₂ and O₂, its large bandgap of 3.2 eV allows it to utilize the UV part of the spectrum, which results in a low spectral utilization. Hence, novel semiconductor materials with lower band gap and efficient charge separation need to be explored as candidates to improve this spectral utilization [20].



In Equation 1, we take the case of a redox reaction of reactant "O" and product "R" at potential V_{redox}° (in volts against the normal hydrogen electrode

(NHE)). This can be measured in terms of energy levels E_{redox} (denoted in electron volts against vacuum) using the relationship as:

$$E_{redox} = constant - eV_{redox}^{\circ} \quad (2)$$

Where the *constant* value is between -4.48 eV and e is the unit charge [21].

The semiconductor catalyst must supply charge carriers that are (i) electrons, at a higher energy level than their reduction level and (ii) holes are supplied lower than the reaction oxidation energy level. Moreover, extra energy is needed to overcome the reaction overpotentials. Hence, using these semiconductor catalysts we can conduct reactions in a non-spontaneous direction by adding irradiant energy and/or electrical energy that can be converted to chemical energy as fuel [21]. This is ideal for the current demand for emission free production methods of chemical synthesis.

1.2. Direct Z-scheme semiconductors

Z-scheme junctions are composite semiconductors that use a two-photon excitation method to achieve higher charge separation similar to photosynthesis in plants. It addresses the issue with single component catalysts like TiO_2 which requires a large bandgap for high charge separation but at the expense of low spectral utilization. These features are mutually exclusive and Z-scheme junctions can in principle overcome this. However, further studies must be carried out to improve their stability, light harvesting, charge separation and transportation to reach economic viability and physical/chemical understanding [22].

Direct Z-scheme semiconductor materials or photosystem (PS-PS) systems are composite semiconductors. This structure is intended to be similar to a tandem solar cell which utilizes junctions of semiconductor materials of different energy band gaps and electron affinities to enhance the solar cell's spectral utilization and produce high voltage outputs i.e. better charge separation. However, in this report, the working of a dual n-type Z-scheme junction is elaborated and is quite different from that of a tandem solar cell.

This paper demonstrates the use of solar cell simulators to model the effectiveness of charge carrier separation in a photocatalyst. The charge carriers are used in the reduction and oxidation sites of the semiconductor catalyst while in a traditional solar cell these carriers contribute directly to electric power generation. Consequently solving the semiconductor equations to describe the carrier kinetics in both systems is equivalent. Moreover, the performance parameters of the photocatalyst as a solar cell will reveal the expectations of the structure under different bias and illumination conditions. This study proposes the use of solar cell simulator SCAPS to simulate direct Z-scheme junctions. For such a Z-scheme heterojunction direct recombination at the interface from both sides needs to be included [23].

It is crucial to engineer photocatalysts that can prevent bulk charge recombination and as such improve the light-harvesting efficiency of the system. Equivalent to thin-film photovoltaic technology, many options to improve water

splitting and CO₂ reduction catalysts have been proposed: bandgap engineering, crystal facet engineering and surface heterojunction optimization [24].

Although characterization of Z-scheme junctions using experimental methods such as photo reduction testing, radical species trapping, metal loading and X-ray photoelectron spectroscopy (XPS) are present [25]. These techniques do not establish a direct link between the experimental parameters and the final device efficiency of converting irradiation to chemical energy. Simulations can address these issues by using the experimental data from characterization and estimating the impact on efficiency by evaluating the charge carrier migration in the photo-catalyst [25].

In this paper, a method to solve the semiconductor equations for a Z-scheme heterojunction is presented. This is done by including defect traps at the interface to allow the photo-generated low energy carriers to recombine, thereby achieving high open circuit voltage (V_{OC}) or charge separation compared to the oxidation or reduction potentials of the desired product.

1.3. Solar Cell Capacitance Simulator (SCAPS)

Solar cell capacitance simulator (SCAPS 1-D) was developed at Ghent University and is available for the research community [26]. It is used to simulate the performance of thin film solar cells and can simulate conventional characterization techniques. The program was developed initially for structures such as CuInSe₂ and CdTe cells, but due to the generality of the semiconductor equations that are solved other structures can be modeled.

The simulator has user-friendly and a graphical interface that gives output data that is useful for the catalyst research and development community. A key reason why SCAPS is used over other solar simulators is because of its ability to include a recombination model based on defects with different properties that are desired in the working of this model and is elaborated further in Section 2.2.

2. Methodology

The primary objective of this study is to evaluate the direct Z-scheme device performance. This is indicated by the efficient conversion of sunlight to electric power or charge carriers that can be used for redox reactions. The three main solar cell parameters used to describe the desired characteristics are:

- the efficiency (η) to indicate the effective conversion of sunlight to generated power.
- current density at maximum power point (J_{MPP}) to indicate the number of carriers to oxidation and reduction sites in the Z-scheme catalyst.
- the voltage at maximum power point (V_{MPP}) is induced potential that indicates whether the reduction and oxidation potentials for the concerning reaction can be exceeded. Higher charge separation is preferred to overcome any overpotentials.

The characteristics and requirements of the catalytic device are similar to those of a solar cell device. This makes solar simulators a viable tool to study the photo, electro or photo electro-catalytic semiconductors.

An established direct Z-scheme junction $\text{TiO}_2/\text{CdIn}_2\text{S}_4$ that is used to reduce and oxidize methyl orange (MO) is used as reference material [27]. It is reported that methyl orange redox potentials are -0.33/2.40 eV (vs. NHE) [27]. The candidate Z-scheme junction should supply a V_{MPP} greater than the difference between the redox potential difference. An overpotential must be added into the redox potential difference for example 0.5 V when using TiO_2 passivated GaP photocatalysts [28]. However, for a prima facie analysis, this is not required and hence omitted in this study.

The (conduction band quasi fermi level) E_{F_N} at the reduction site must be higher than the reduction potential of the reaction and the (valence band quasi fermi level) E_{F_P} at the oxidation site must be lower than the oxidation reaction. This will help in evaluating the feasibility of charge carriers to move from the semiconductor material and take part in the chemical reaction. This is similar to the metalwork function of a contact in a solar cell and electron or hole transport layer. It is reported that the TiO_2 and CdIn_2S_4 have E_{CB}/E_{VB} levels at -0.29/2.91 eV and -0.82/1.38 eV (vs. NHE) which are the material parameters implemented in SCAPS as input parameters [27]. Since the energy levels meet the primary criteria, they can be considered good candidates for a Z-scheme junction for methyl orange oxidation and reduction catalysis.

Bard et al. state that the properties of the electrolyte can also be modeled as an intrinsic semiconductor with specific parameters [21]. Such an approximation is not experimentally validated in combination with a Z-scheme, therefore this is not included in our proposed model in this paper. This can be proposed as future work. This paper will focus on modeling the Z-scheme junction.

2.1. Numerical modeling of semiconductor devices

Partial differential equations are used to model the behavior of charge carriers in semiconductor devices [29].

Poisson's equation in the one-dimensional case is written as:

$$\frac{d^2\psi}{dx^2} = \frac{dE}{dx} = -\frac{q}{\epsilon}[N(x) + p - n] \quad (3)$$

Where ψ stands for the potential, E stands for the electric field, x for the position, $N(x)$ is the net charge concentration of the impurities or dopants, q is the electronic charge, ϵ is the dielectric constant of the semiconductor layer, p and n are the hole and electron densities, respectively. The charge carrier concentration in the semiconductor is evaluated using the continuity equations at steady state conditions across the cell thickness as:

$$\begin{aligned} \frac{1}{q} \frac{dJ_n}{dx} &= U - G \\ \frac{1}{q} \frac{dJ_p}{dx} &= -(U - G) \end{aligned} \quad (4)$$

Table 1: Semiconductor layer parameters used in this study.

	PS I	PS II
Material	TiO ₂	CdIn ₂ S ₄
Thickness [μm]	2	2
Bandgap [eV]	3.2	2.2
Electron affinity [eV]	5.81	4.78
Dielectric permittivity	10	10
CB effective density of states [$10^{19} \text{ cm}^3/\text{s}$]	1	1
VB effective density of states [$10^{19} \text{ cm}^3/\text{s}$]	1	1
Electron thermal velocity [10^7 cm/s]	1	1
Hole thermal velocity [10^7 cm/s]	1	1
Electron mobility [$\text{cm}^2/\text{V s}$]	50	50
Hole mobility [$\text{cm}^2/\text{V s}$]	50	50
Shallow uniform donor density (N_D) [10^{12} 1/cm^3]	1	9000
Shallow uniform acceptor density (N_A) [$1/\text{cm}^3$]	10	10
Radiative recombination coefficient [$10^{-4} \text{ cm}^3/\text{s}$]	1	1

Table 2: Interface layer parameters used in this study are assumed. σ is capture cross-section.

Parameter type	Value
Defect type	Neutral
σ_e [10^{-19} cm^2]	1
σ_h [10^{-19} cm^2]	1
Energetic distribution	Single
Reference for defect energy level (E_t)	Above middle of interface gap
Energy with respect to Reference [eV]	0
Total density [10^{10} 1/cm^2]	1

Where J_n and J_p represent the current densities by electrons and holes, respectively. U and G are the recombination and generation rates, respectively [30].

In Table 1, the semiconductor parameters are shown in this model to study the Z-scheme device [27]. In Table 2, the interface properties were given.

The left and right contacts are simulated to have flat bands with electron and hole surface recombination rates of 10^5 and 10^7 cm/s respectively.

2.2. Shockley Read Hall (SRH) recombination at the interface

It is assumed that the low-energy charge carrier recombination at the interface between the layers of the Z-scheme semiconductor is due to the presence of high defect densities. In SCAPS, the proposed recombination can be modeled in the form of SRH recombination at a particular energy state. It is reported that the recombination at these interface defects can be modeled using SRH recombination. This type of recombination path was introduced in SCAPS to

model polycrystalline solar cells such as the interface between CdS/CdTe cells [26].

Many solar cell simulators only treat SRH recombination within the same layer and require a dummy layer in between to handle this. This SRH recombination path from both sides of the interface will be utilized in the Z-scheme model for which low energy carriers from both materials can directly recombine via the interface states.

2.3. Energy band diagram of the Z-scheme heterojunction

Z-scheme junctions require a particular characteristic in their energy band diagram.

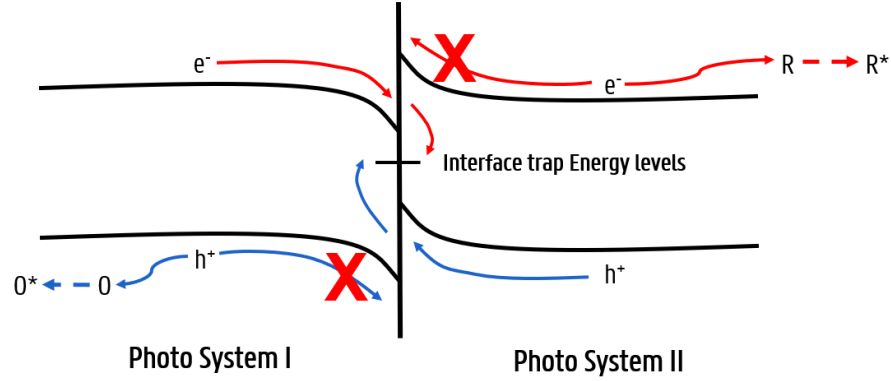


Figure 1: A schematic in the charge carrier propagation in a direct Z-scheme junction. The red line indicates the motion of electrons (e^-) and the blue line indicates the motion of holes (h^+).

Figure 1 illustrates that the valence band in Photosystem I (PS I) layer is required to hold the high energy holes generated to be utilized in the oxidation site, hence an energy barrier must be present. The high energy holes are moved to the oxidation sites where the oxidation reactant O gives an electron to the semiconductor catalyst, forming the oxidized product O^* . The conduction band in Photosystem II (PS II) layer is required to hold the high energy electrons generated to be utilized in the reduction site, hence an energy barrier must be present. The high energy electrons are moved to the reduction sites where the reduction reactant R takes an electron from the semiconductor catalyst, forming the oxidized product R^* . The low energy charge carriers of PS I and PS II are electrons and holes, respectively. They recombine due to the interface states present. This is illustrated in the presence of the valence band and conduction band energy dips.

In the case of the $TiO_2/CdIn_2S_4$ Z-scheme junction which is modeled in this study. The illumination of AM1.5 1 sun spectrum is falling on the TiO_2 layer first. TiO_2 layer is PS I and the $CdIn_2S_4$ layer is PS II in this study.

The recombination at the interface is modeled in SCAPS using defects at trap energy levels between the PS I and PS II conduction and valence band edges.

A direct Z-scheme heterojunction model is developed to resemble the working of a Z-scheme junction in a solar cell simulator such as SCAPS. The recombination of low energy charge carriers is simulated using SRH recombination of these carriers in neutral defects in the interface between the two semiconductor layers.

2.4. Model validation

Open circuit voltage or V_{OC} of the semiconductor device is the direct measurement of the charge separation capability. The reduction and oxidation capability of the catalyst is proportional to the V_{OC} . The short circuit current or J_{SC} of the semiconductor is an important characteristic to note as well, as it quantifies the amount of high energy charge carriers that are available at the reduction and oxidation sites. The efficiency translates to the utilization of solar irradiation by the material.

To evaluate whether the modeled structure is a Z-scheme junction the current that should be matched in both photosystems should cross the interface via recombination. In such a situation, the ideal case is when low-energy charge carriers recombine at the interface and the high-energy charge carriers exit the device into the contacts, where they can be used for reduction and oxidation.

3. Results and Discussion

SCAPS models the Z-scheme junction at a given irradiation and gives the corresponding current density-voltage (JV) curve. The solar cell parameters are estimated using this JV curve. The energy bands can be simulated at a given voltage. It is useful in establishing whether the junction modeled is indeed a Z-scheme junction.

3.1. Energy band diagram

The energy band diagram of the modeled Z-scheme junction is given in Figure 2. The charge carriers must be at the energy levels that are required for the redox reactions to occur. It must be noted that a Z-scheme junction also has a distinct energy band diagram with barriers at the interface to facilitate the recombination of low-energy carriers and to hold the high-energy carriers to be supplied to the respective reaction sites [13].

Figure 2 illustrates the energy band diagram of the $TiO_2/CdIn_2S_4$ with respect to the fermi level (E_F) of neutral TiO_2 . On the left side of the device, we have the TiO_2 layer with its distinctive high energy gap and higher electron affinity. On the right side, we have the $CdIn_2S_4$ layer with a lower energy gap and lower electron affinity.

It is noted that the band bending generated in the simulated materials is that of the direct Z-scheme as the energy barriers in the PS II ($CdIn_2S_4$ layer) conduction band keeps the electrons at high energy and can be used in the

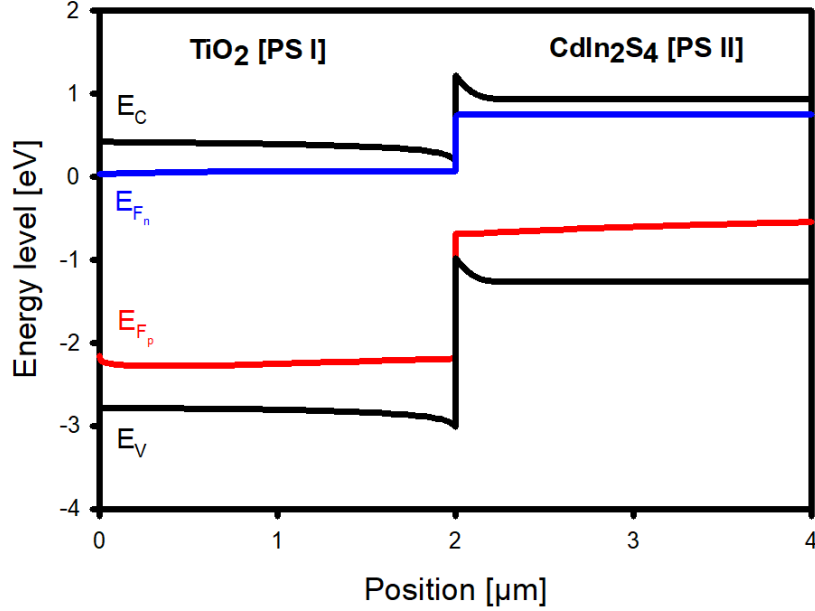


Figure 2: Energy band diagram of the $\text{TiO}_2/\text{CdIn}_2\text{S}_4$ Z-scheme junction in SCAPS with respect to the fermi level E_F of neutral TiO_2 (0.4175 eV wrt. vacuum) at the illumination of 1000 W/m^2 and 0 V.

reduction sites. The same can be concluded for the valence band of PS I (TiO_2 layer) for holes that can be supplied to the oxidation sites. This confirms that the established $\text{TiO}_2/\text{CdIn}_2\text{S}_4$ Z-scheme junction shows the modeled energy band diagram which is desired for a Z-scheme junction.

Figure 3 illustrates the calculated charge carrier concentration in the modeled Z-scheme device. The specific band offset results in an increased concentration of electrons and holes close to the interface ($x = 2 \mu\text{m}$). The high charge concentrations facilitate a high recombination rate for electrons in PS I and holes in PS II.

The recombination at the interface is signified by the high peaks and troughs formed at the interface between the PS I and PS II layers of the Z-scheme junction at the interface at $2 \mu\text{m}$ (total thickness $4 \mu\text{m}$). For equivalent capture cross-sections of the interface defects, the capture rate is proportional to the carrier concentration at the interface and thus capture of electrons from PS I and holes from PS II will be the most important terms in the SRH mechanism. Defects are present at the trap energy level between the conduction band of TiO_2 and the valence band of CdIn_2S_4 . The low-energy charge carriers shall meet up at these defect sites and undergo SRH recombination.

SCAPS then simulates the JV curve of the device and calculates the device

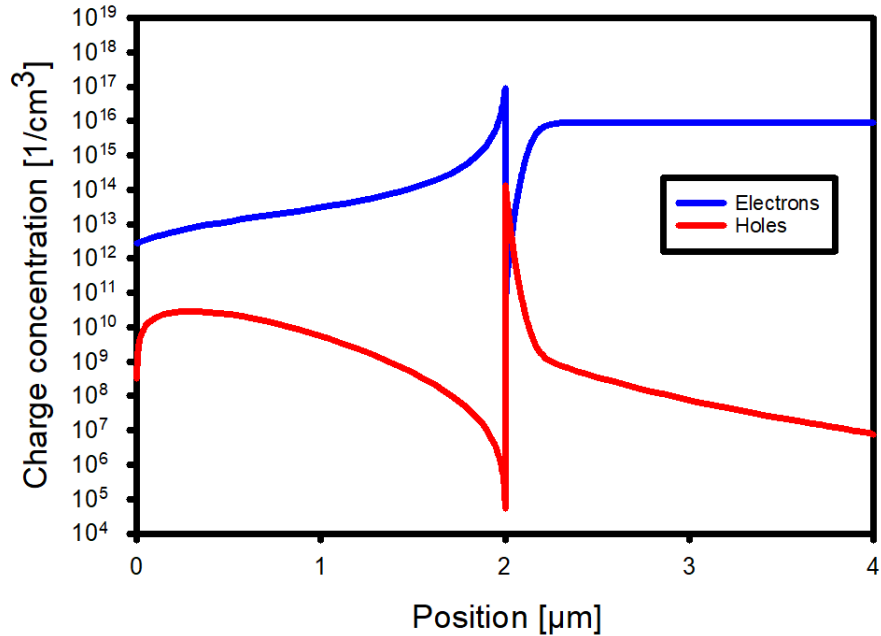


Figure 3: Hole and electron concentration across the modeled Z-scheme device thickness in red and blue line, respectively from SCAPS model at 1000 W/m^2 and 0 V .

performance parameters as in Figure 4. In this case, the corresponding solar cell parameters are shown in Table 3. It can be seen that the JV curve of this modeled Z-scheme device is unlike an efficient solar cell Z-scheme curve where the open circuit voltage is made to work very close to the maximum power point. This can be attributed to the low fill factor (FF) of the heterojunction. FF is defined as the ratio between the maximum power density of the device which is the green area and the product of V_{OC} and J_{SC} which is the grey area in Figure 4.

The low fill factor compared to that observed in solar cells is because unlike in solar cells where the objective is to collect maximum number of charge carriers at contacts for electrical power generation. The objective of a direct Z-scheme device used in catalysis would be maximum charge separation. This would be possible with the low energy charge carriers recombining and thereby utilizing high energy charge carriers for power generation or reduction/oxidation catalysis.

3.2. Defect density effect

The defect densities at the interface play an important role in the model as they provide the recombination levels for the recombination junction in between

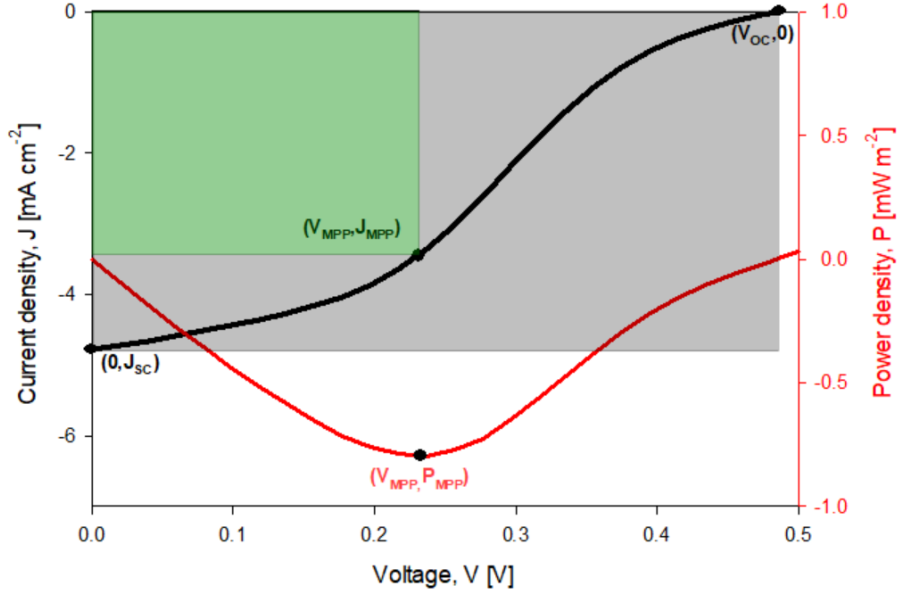


Figure 4: SCAPS current density vs. voltage characteristics (JV curve) in black and Power density vs. voltage in red on applying AM1.5 solar spectrum on $\text{TiO}_2/\text{CdIn}_2\text{S}_4$ Z-scheme junction. With illumination on the right side (TiO_2 side). The grey area indicates $V_{OC} \times J_{SC}$ and the green area is $V_{MPP} \times J_{MPP}$ which is P_{MPP} ie., maximum power density.

the photosystems for the device which is the interface. By increasing the density of these trap defects, there are more sites for the low energy charge carriers to occupy for recombination as illustrated in Figure 1. This will allow the high energy charge carriers to be separated and utilized for reduction and oxidation reactions. It is investigated if the type of defect (neutral, acceptor or donor) has a role in the cell performance as well. Figure 5 illustrates that there is a direct correlation between the total defect density at the interface and the performance of the solar cell parameters. As the total defect density is increased, there is an increase in all cell parameters as cell efficiency (η), V_{OC} , J_{SC} and FF.

A key takeaway here is that the number of recombination sites increases at the interface, the cell parameters of the Z-scheme junction improves with better charge separation and better charge density at the oxidation and reduction sites.

The effect of the type of defect is shown above in Figure 6. The acceptor or donor nature of the defect type was found to have no profound effect on the model characteristics as the cell parameters showed little to no variation. There is consistent overlapping of the Z-scheme JV curves for different defect types. This indicates that the charge of the interface defects has a negligible impact on the interface recombination rate and efficiency of the device as well.

Table 3: SCAPS device parameters of the simulated $\text{TiO}_2/\text{CdIn}_2\text{S}_4$ Z-scheme junction from the JV curve in Figure 4.

Parameters	Unit	Value
Open circuit voltage, V_{OC}	[mV]	480
Short circuit current, J_{SC}	[mA/cm ²]	4.78
Fill factor, FF	[%]	34.32
Efficiency, η	[%]	0.79
Voltage at maximum power point, V_{MPP}	[V]	0.23
Current at maximum power point, J_{MPP}	[mA/cm ²]	3.44

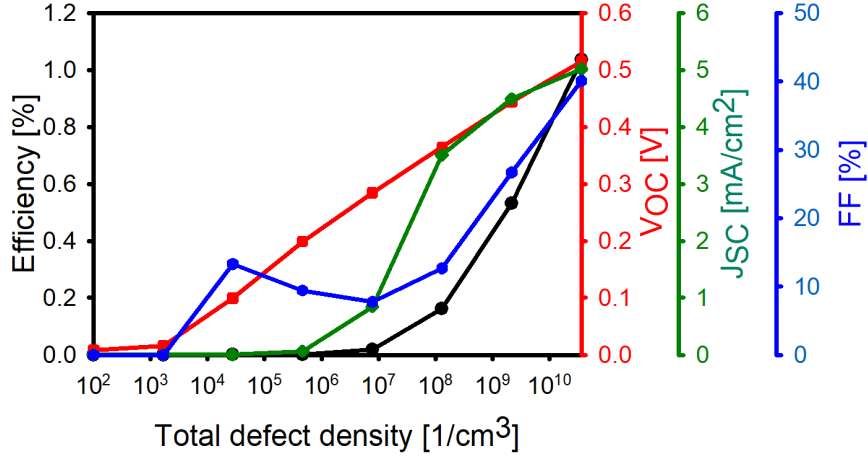


Figure 5: Solar cell parameters plotted as a function of the total defect density at the interface from SCAPS. The cell efficiency (η) is indicated in black, the open circuit voltage (V_{OC}) is indicated in red, the short circuit current (J_{SC}) is indicated in green and the fill factor (FF) is indicated in blue.

3.3. Band offsets effect

In the previous section, it is shown that the recombination at the interface has a direct correlation with the performance of the device. One can study the influence of the energy barriers and dips can have on the Z-scheme device using solar simulators. It is noted that these barriers help in isolating the high-energy charge carriers from the low-energy charge carriers. The dips in the energy band diagram in Figure 2 will help the recombination of the low-energy charge carriers. To study the influence of these band offsets, the PS I remained constant the energy position of the band edges of PS II are varied. Two options are described below.

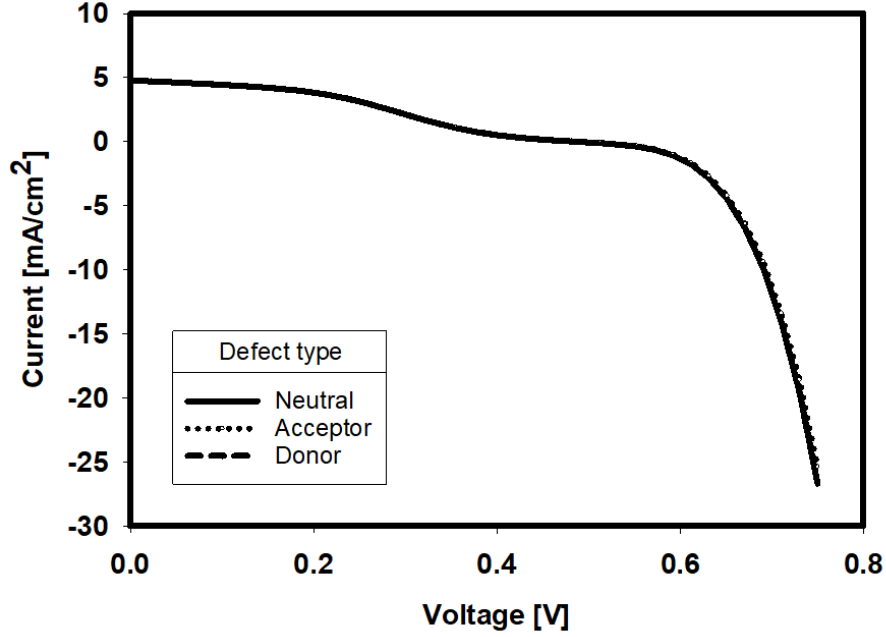


Figure 6: Effect of defect type being "neutral" i.e, a hypothetical center carrying no charge, donor or acceptor on the JV curve of the simulated Z-scheme device from SCAPS.

3.3.1. Fixed PS II conduction band

The conduction band of PS II is fixed at 4.78 eV which is the electron affinity of the CdIn_2S_4 material. The PS II energy gap is varied from 1 eV to 3 eV which changes the valence band position with respect to the conduction band in the model. The solar cell performance parameters as a function of PS II energy gap is shown in Figure 7.

Figure 7 illustrates the effect of the energy gap of PS II on the performance of the Z-scheme junction with fixed PS II conduction band. Device efficiency increases to a maximum of about 1.5% at about 1.1 eV and then decreases as the energy gap is increased. An irregularity in the fill factor (FF) and V_{OC} curve close to 1.5 eV can also be noticed. For these band offsets, convergence failure occurred in SCAPS induced by the high free carrier concentrations at the interface.

The efficiency curve can be explained as it follows the V_{OC} trend initially till the rise to maxima and then the J_{SC} trend during its fall with an increase in the energy gap (E_g) of the photosystem II (PS II) semiconductor layer.

When the bandgap energy (E_g) of PS II is 1 eV, the conduction band edge of PS I with respect to vacuum is at 5.81 eV (electron affinity (X) of PS I) and the valence band of PS II is $X + E_g$ i.e. 5.78 eV. It means that the valence band edge of PS II is above the conduction band edge of PS I by about 0.03 eV.

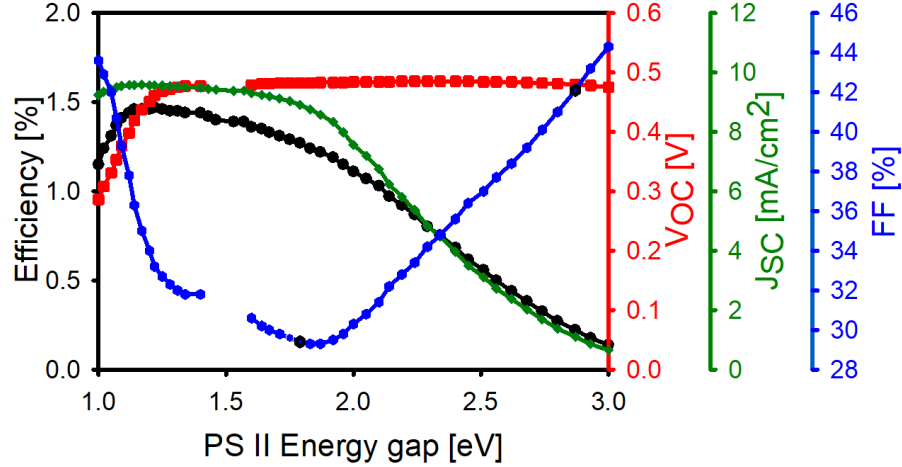


Figure 7: The solar cell parameters as a function of the PS II Energy bang gap from SCAPS model. The cell efficiency (η) is indicated in black, the open circuit voltage (V_{OC}) is indicated in red the short circuit current (J_{SC}) is indicated in green and the fill factor (FF) is indicated in blue. Results obtained from the SCAPS model.

This leads to a structure with no interface band gap with a high concentration of low energy carriers and there will be no interface recombination occurring due to the interface defects. As the E_g of PS II is increased, the interface gap increases. This leads to the defects being utilized for the low energy charge carriers recombination. As the energy gap is increased further, the charge carrier generation is dropped as a lower number of photons is absorbed in the PS II layer due to its large bandgap. The model is able to predict an optimal structure when the energy gap of PS II is 1.1 eV.

3.3.2. Fixed PS II valence band

The valence band is fixed by making sure that the sum of electron affinity and energy gap is constant. The energy position of the valence band corresponds with the values in Table 1. Parameter sweeps are conducted for values of PS II E_a and PS II E_g where the sum stays 6.98 eV. The results of the parameter sweep is shown in the Figure 8 as a function of the PS II energy gap.

As the PS II energy gap is increased from 1.0 to 1.69 eV. The device shows little to no performance as the PS II conduction band is below the conduction band of the PS I. Therefore, there is no barrier for electrons generated and the recombination mechanism at the interface is not the preferential mechanism for carrier collection. As the PS II energy gap is further increased which means the electron affinity of PS II is decreasing. The PS II conduction band continues to move away from the PS I conduction band making a positive band offset in the conduction band from PS I to PS II. This barrier keeps the high energy charge carriers from going to a low energy level and allows the recombination of

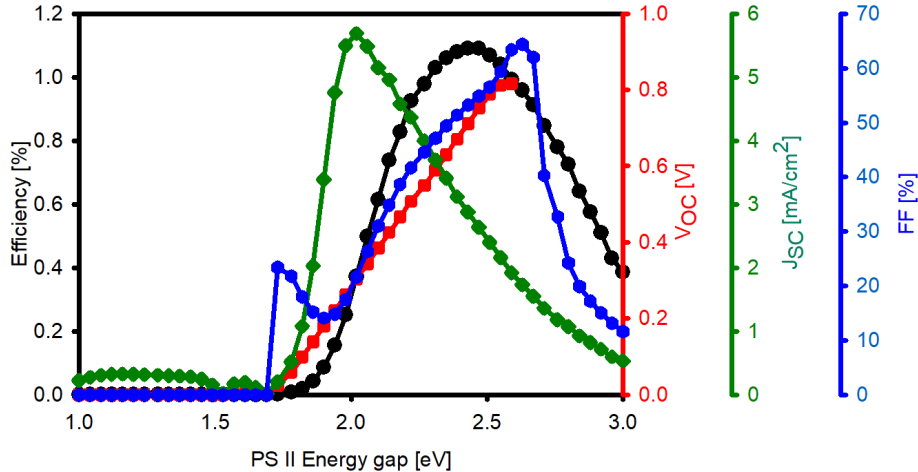


Figure 8: The solar cell parameters as a function of the PS II energy gap from SCAPS model. Where the PS II satisfies the condition that the sum of the energy gap and electron affinity is 6.98 eV. The cell efficiency (η) is indicated in black, the open circuit voltage (V_{OC}) is indicated in red the short circuit current (J_{SC}) is indicated in green and the fill factor (FF) is indicated in blue. Results obtained from the SCAPS model.

low energy charge carriers. On the other hand, when the energy gap is further increased. The generation of carriers in PS II will reduce. Hence, there is a maximum in the device efficiency. The efficiency curve rises to a maxima of 1.09% at PS II energy gap of 2.43 eV. The only performance parameter that gradually rises is the V_{OC} due to the rise in the built-in potential in the junction. The absence of data points beyond 2.6 eV is due to convergence failures occurring in SCAPS when calculating the open circuit potential for these points.

4. Conclusion

Z-scheme semiconductor materials have desirable optoelectrical properties that make them viable chemical catalysts for reduction and oxidation reactions. As there are various combinations of semiconductor layers possible for this composite material, the development of a screening model was imperative to evaluate the feasibility of the material and the desired application. It can be used as a primary study tool to evaluate various semiconductor candidates that can be used for charge carrier generation for chemical reduction and oxidation.

It is concluded that solar cell simulators such as SCAPS are powerful tools to assess Z-scheme junctions. Its user-friendly interface is beneficial in reducing the learning curve for the catalyst research community. The cell parameters can help in giving a prima-face analysis of the feasibility of using certain materials as a catalyst.

The modeling methodology of a direct Z-scheme junction using a solar cell simulator (SCAPS) is presented in this study. The key performance indicators are presented along with an example case using an established junction ($\text{TiO}_2/\text{CdIn}_2\text{S}_4$). A direct correlation between the recombination of low-energy carriers at the interface and device performance is presented.

Data availability

Data will be available from the corresponding author upon reasonable request.

References

- [1] F. D. Meylan, V. Moreau, S. Erkman, [CO₂ utilization in the perspective of industrial ecology, an overview](#), Journal of CO₂ Utilization 12 (2015) 101–108. doi:10.1016/j.jcou.2015.05.003. URL <http://dx.doi.org/10.1016/j.jcou.2015.05.003>
- [2] R. M. Cuéllar-Franca, A. Azapagic, Carbon capture, storage and utilisation technologies: A critical analysis and comparison of their life cycle environmental impacts, Journal of CO₂ Utilization 9 (2015) 82–102. doi:10.1016/j.jcou.2014.12.001.
- [3] Y. Wang, D. He, H. Chen, D. Wang, Catalysts in electro-, photo- and photoelectrocatalytic CO₂ reduction reactions, Journal of Photochemistry and Photobiology C: Photochemistry Reviews 40 (2019) 117–149. doi:10.1016/j.jphotochemrev.2019.02.002.
- [4] R.-P. Ye, J. Ding, W. Gong, M. D. Argyle, Q. Zhong, Y. Wang, C. K. Russell, Z. Xu, A. G. Russell, Q. Li, et al., CO₂ hydrogenation to high-value products via heterogeneous catalysis, Nature communications 10 (1) (2019) 5698.
- [5] A. Fujishima, K. Honda, [Electrochemical photolysis of water at a semiconductor electrode](#), Nature 238 (1972) 37–38. doi:10.1038/238037a0. URL <https://doi.org/10.1038/238037a0>
- [6] F. Zhang, X. Wang, H. Liu, C. Liu, Y. Wan, Y. Long, Z. Cai, Recent advances and applications of semiconductor photocatalytic technology, Applied Sciences (Switzerland) 9 (2019). doi:10.3390/app9122489.
- [7] Y. Horie, D. A. David, M. Taya, S. Tone, [Effects of light intensity and titanium dioxide concentration on photocatalytic sterilization rates of microbial cells](#), Industrial & Engineering Chemistry Research 35 (1996) 3920–3926, doi: 10.1021/ie960051y. doi:10.1021/ie960051y. URL <https://doi.org/10.1021/ie960051y>

- [8] C. Jin, X. Liu, L. Tan, Z. Cui, X. Yang, Y. Zheng, K. W. K. Yeung, P. K. Chu, S. Wu, [Ag/AgBr-loaded mesoporous silica for rapid sterilization and promotion of wound healing](#), *Biomaterials Science* 6 (2018) 1735–1744. doi:10.1039/C8BM00353J. URL <http://dx.doi.org/10.1039/C8BM00353J>
- [9] R. Wang, W. Zhang, W. Zhu, L. Yan, S. Li, K. Chen, N. Hu, Y. Suo, J. Wang, [Enhanced visible-light-driven photocatalytic sterilization of tungsten trioxide by surface-engineering oxygen vacancy and carbon matrix](#), *Chemical Engineering Journal* 348 (2018) 292–300. doi:https://doi.org/10.1016/j.cej.2018.05.010. URL <https://www.sciencedirect.com/science/article/pii/S138589471830799X>
- [10] C. S. Praveen, *Semiconductors as catalysts for water*, Materials Research Laboratory (2012).
- [11] Q. Li, B. Guo, J. Yu, J. Ran, B. Zhang, H. Yan, J. R. Gong, [Highly efficient visible-light-driven photocatalytic hydrogen production of CdS-cluster-decorated graphene nanosheets](#), *Journal of the American Chemical Society* 133 (2011) 10878–10884, doi: 10.1021/ja2025454. doi:10.1021/ja2025454. URL <https://doi.org/10.1021/ja2025454>
- [12] R. Wang, S. Ni, G. Liu, X. Xu, [Hollow CaTiO₃/La/Cr co-doping for efficient photocatalytic hydrogen production](#), *Applied Catalysis B: Environmental* 225 (2018) 139–147. doi:https://doi.org/10.1016/j.apcatb.2017.11.061. URL <https://www.sciencedirect.com/science/article/pii/S092633731731127X>
- [13] L. Chen, Y. Qin, G. Chen, M. Li, L. Cai, Y. Qiu, H. Fan, M. Robert, T.-C. Lau, [A molecular noble metal-free system for efficient visible light-driven reduction of CO₂ to CO](#), *Dalton Transactions* 48 (2019) 9596–9602. doi:10.1039/C9DT00425D. URL <http://dx.doi.org/10.1039/C9DT00425D>
- [14] W. Tan, B. Cao, W. Xiao, M. Zhang, S. Wang, S. Xie, D. Xie, F. Cheng, Q. Guo, P. Liu, [Electrochemical reduction of CO₂ on hollow cubic Cu₂O@Au nanocomposites](#), *Nanoscale Research Letters* 14 (2019) 63. doi:10.1186/s11671-019-2892-3. URL <https://doi.org/10.1186/s11671-019-2892-3>
- [15] D. Vidyasagar, N. Manwar, A. Gupta, S. G. Ghugal, S. S. Umare, R. Boukherroub, [Phenyl-grafted carbon nitride semiconductor for photocatalytic CO₂-reduction and rapid degradation of organic dyes](#), *Catalysis Science & Technology* 9 (2019) 822–832. doi:10.1039/C8CY02220H. URL <http://dx.doi.org/10.1039/C8CY02220H>

- [16] Q. Liu, Y. Zhou, J. Kou, X. Chen, Z. Tian, J. Gao, S. Yan, Z. Zou, [High-yield synthesis of ultralong and ultrathin \$\text{Zn}_2\text{GeO}_4\$ nanoribbons toward improved photocatalytic reduction of \$\text{CO}_2\$ into renewable hydrocarbon fuel](#), Journal of the American Chemical Society 132 (2010) 14385–14387, doi: 10.1021/ja1068596. doi:10.1021/ja1068596. URL <https://doi.org/10.1021/ja1068596>
- [17] Y. Boyjoo, H. Sun, J. Liu, V. K. Pareek, S. Wang, A review on photocatalysis for air treatment: From catalyst development to reactor design, Chemical engineering journal 310 (2017) 537–559.
- [18] X. Fu, W. A. Zeltner, M. A. Anderson, Applications in photocatalytic purification of air, Studies in surface science and catalysis 103 (1997) 445–461.
- [19] A. S. Besov, A. V. Vorontsov, V. N. Parmon, Fast adsorptive and photocatalytic purification of air from acetone and dimethyl methylphosphonate by TiO_2 aerosol, Applied Catalysis B: Environmental 89 (2009) 602–612.
- [20] N. Serpone, A. V. Emeline, Semiconductor photocatalysis - past, present, and future outlook, Journal of Physical Chemistry Letters 3 (2012) 673–677. doi:10.1021/jz300071j.
- [21] A. J. Bard, Photoelectrochemistry and heterogeneous photo-catalysis at semiconductors, Journal of Photochemistry 10 (1979) 59–75. doi:10.1016/0047-2670(79)80037-4.
- [22] P. Zhou, J. Yu, M. Jaroniec, All-solid-state z-scheme photocatalytic systems, Advanced Materials 26 (2014) 4920–4935. doi:10.1002/adma.201400288.
- [23] H. Pauwels, G. Vanhoutte, The influence of interface state and energy barriers on the efficiency of heterojunction solar cells, Journal of Physics D: Applied Physics 11 (5) (1978) 649.
- [24] D. Huang, S. Chen, G. Zeng, X. Gong, C. Zhou, M. Cheng, W. Xue, X. Yan, J. Li, [Artificial z-scheme photocatalytic system: What have been done and where to go?](#), Coordination Chemistry Reviews 385 (2019) 44–80. doi:10.1016/j.ccr.2018.12.013. URL <https://doi.org/10.1016/j.ccr.2018.12.013>
- [25] J. Low, C. Jiang, B. Cheng, S. Wageh, A. A. Al-Ghamdi, J. Yu, A review of direct z-scheme photocatalysts, Small Methods 1 (2017) 1–21. doi: 10.1002/smtd.201700080.
- [26] M. Burgelman, P. Nollet, S. Degraeve, [Modelling polycrystalline semiconductor solar cells](#), Thin Solid Films 361-362 (2000) 527–532. doi: 10.1016/S0040-6090(99)00825-1. URL <https://scaps.elis.ugent.be/>

- [27] Y. Chen, Q. Hu, M. Yu, X. Gong, S. Li, S. Wang, H. Yu, Z. Li, In-situ construction of a direct z-scheme $\text{CdIn}_2\text{S}_4/\text{TiO}_2$ heterojunction for improving photocatalytic properties, *CrystEngComm* 23 (2021) 5070–5077. [doi:10.1039/D1CE00338K](https://doi.org/10.1039/D1CE00338K).
- [28] G. Zeng, J. Qiu, Z. Li, P. Pavaskar, S. B. Cronin, CO_2 reduction to methanol on TiO_2 -passivated GaP photocatalysts, *ACS Catalysis* 4 (10) (2014) 3512–3516.
- [29] W. Shockley, *Electrons and holes in semiconductors: with applications to transistor electronics*, van Nostrand, 1959.
- [30] P. A. Basore, Numerical modeling of textured silicon solar cells using pc-1d, *IEEE Transactions on Electron Devices* 37 (1990) 337–343. [doi:10.1109/16.46362](https://doi.org/10.1109/16.46362).

Acknowledgments

The authors would like to acknowledge Catalisti for their funding through the Moonshot SYN-CAT project. The funder played no role in the study design, data collection, analysis and interpretation of data, or the writing of this manuscript. The cooperation of the consortium partners is acknowledged and appreciated.

Author contributions

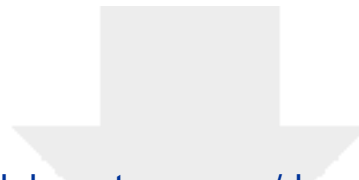
JoL conceived the original idea. NTJ and JoL developed and modeled the Z-scheme junction. They were the major contributors to the writing of the manuscript. BV, JoL and JeL provided expert insights and were involved in the proofreading of the manuscript. BV and JoL secured funding for this project. All authors read and approved the final manuscript.

Competing interests

The authors declare no competing financial or non-financial interests.

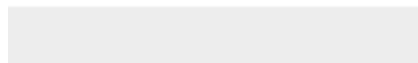
Additional information


Correspondence and requests for materials should be addressed to Nithin Thomas Jacob and Johan Lauwaert.



[Click here to access/download](#)

Supplementary and Electronic files
Supplementary.docx





[Click here to access/download](#)

LaTeX Source Files
Solar Energy.zip



Declaration of interests

☒ The authors declare that they have no known competing financial interests or personal relationships that could have appeared to influence the work reported in this paper.

☐ The authors declare the following financial interests/personal relationships which may be considered as potential competing interests: